

**ZERO SEQUENCE CURRENTS IN AC LINES
CAUSED BY
TRANSIENTS IN ADJACENT DC LINES**

by

Naresh K. Chopra

**A thesis
submitted to
the Faculty of Graduate Studies
in Partial Fulfilment of the Requirements
for the Degree of Master of Science**

Department of Electrical Engineering

UNIVERSITY OF MANITOBA



Winnipeg, Manitoba, Canada

August 1986

Permission has been granted to the National Library of Canada to microfilm this thesis and to lend or sell copies of the film.

The author (copyright owner) has reserved other publication rights, and neither the thesis nor extensive extracts from it may be printed or otherwise reproduced without his/her written permission.

L'autorisation a été accordée à la Bibliothèque nationale du Canada de microfilmer cette thèse et de prêter ou de vendre des exemplaires du film.

L'auteur (titulaire du droit d'auteur) se réserve les autres droits de publication; ni la thèse ni de longs extraits de celle-ci ne doivent être imprimés ou autrement reproduits sans son autorisation écrite.

ISBN 0-315-33941-1

ZERO SEQUENCE CURRENTS IN AC LINES CAUSED BY
TRANSIENTS IN ADJACENT DC LINES

BY

NARESH K. CHOPRA

A thesis submitted to the Faculty of Graduate Studies of
the University of Manitoba in partial fulfillment of the requirements
of the degree of

MASTER OF SCIENCE

© 1986

Permission has been granted to the LIBRARY OF THE UNIVERSITY OF MANITOBA to lend or sell copies of this thesis, to the NATIONAL LIBRARY OF CANADA to microfilm this thesis and to lend or sell copies of the film, and UNIVERSITY MICROFILMS to publish an abstract of this thesis.

The author reserves other publication rights, and neither the thesis nor extensive extracts from it may be printed or otherwise reproduced without the author's written permission.

ABSTRACT

This thesis examines the induction effects in a multiconductor system with ground return. It is shown that a strong coupling exists between the lines with ground return at low frequencies even if the lines are considerably apart. The motivation for studying this phenomenon came from an unexplained tripping of 230 kV ac lines during one of the tests conducted by Manitoba Hydro, involving parallel operation of two of its dc poles.

In order to study the phenomenon associated with this problem, a simple but sufficient transmission line model was developed. A digital simulation program was written to simulate the system under various conditions. A parametric study was carried out to examine the effects of different parameters involved in the system such as frequency, ground resistivity etc. on the induction between the two lines. It is shown that large zero sequence currents can be induced in the ac line due to transients in the nearby dc lines. The phenomenon involved is explained both mathematically and qualitatively.

Methods to protect against such large zero sequence currents in ac lines have also been outlined.

ACKNOWLEDGEMENTS

The author is grateful to the Manitoba Hydro Research Committee for funding this project. The author also wishes to thank Dr. J. Chand and Mr. R. W. Haywood of the staff of the System Performance section with whom he had useful discussions from time to time.

A very special word of thanks is reserved for Professor A. Gole, the author's supervisor, who always lent support, and provided his expertise and incisive suggestions towards the completion of this report. The author has benefited immensely from his association with Dr. Gole and will appreciate such a relationship for many years to come.

The author expresses deep gratitude to Professor L. M. Wedepohl of The University of British Columbia with whom the author collaborated on the modelling aspects, which proved to be of immense help. Appreciation also goes to Greg Bridges and to my other colleagues for the useful discussions the author had with them.

Table of Contents

Abstract	i
Acknowledgement	ii
Table of Contents	iii
List of symbols	v

Chapter	Page
Chapter 1. Introduction	1
Chapter 2. Line Parameter Calculations of a Multiconductor System	
2.1 General	7
2.2 Transmission Line Differential Equations	8
2.3 Modelling of the Transmission Line	9
2.4 Calculation of Impedance Matrix	11
2.4.1 Calculation of Self Impedance	11
2.4.2 Calculation of Mutual Impedance	17
2.5 Calculation of the Admittance Matrix	19
2.6 Elimination of Ground Wires	21
Chapter 3. Solution of Transmission Line Differential Equations for a Multiconductor System	
3.1 Introduction	25
3.2 Solution Transmission Line Differential Equations	25
3.2.1 Propagation of Voltage	26
3.2.2 Propagation of Current	31
3.3 Multiconductor System as a Two-Port Network	32

3.4	An example	36
Chapter 4.	Parametric Study on a simplified Multiconductor System with Ground Return	
4.1	Introduction	42
4.2	Digital Simulation of a Multiconductor System with Ground Return	44
4.3	Testing of Digital Simulation Program	47
4.4	Parametric Studies of the Model	50
4.4.1	Base Case	50
4.4.2	Effect of Ground Resistivity	52
4.4.3	Effect of varying distance between the lines (ac and dc)	58
4.4.4	Effect of Contact Resistance	60
4.4.5	Effect of mutual Contact Resistance	64
4.4.6	Effect of Ground Wires	67
4.5	System Response with time domain input signal	70
Chapter 5.	Conclusions and Recommendations	75
References		79
Appendix-I		

LIST OF SYMBOLS

Some of the frequently occurring symbols in this thesis are tabulated below.

V	phasor voltage
I	phasor current
Z	impedance matrix
Y	admittance matrix
$\rho_{i,j}$	resistivity of conductor i or j
ρ	ground resistivity
de	depth of penetration of current into ground ($= \sqrt{\frac{\rho}{j\omega\mu}}$)
$r_{i,j}$	radius of conductor i or j
$h_{i,j}$	height of conductor i or j above ground
A	product of Z and Y matrices
λ_s	eigenvalues of matrix A
$E_v s$	eigenvectors of matrix A
γ	propagation constant
f	frequency
μ_0	permeability of air
ϵ_0	permittivity of air

CHAPTER 1

INTRODUCTION

During the summer of 1985, Manitoba Hydro conducted a number of tests to check the parallel operation of two of its dc poles. One of the tests which involved the blocking and bypassing of two parallel poles resulted in tripping of three 230 kv ac lines coming from the Grand Rapids generating station of Manitoba Hydro. These lines which run adjacent to the dc lines for a distance of approximately 240 kilometres, were tripped due to the operation of the zero sequence current relays at the line terminations. A schematic diagram of the system and the concerned lines at the time of the test is shown in Fig.(1.1). Fortunately the trippings did not cause any serious problem due to small line loadings. But the similar disturbances at heavier line loadings would have the potential of system break up and loss of load in the system.

An analysis of the disturbances (Appendix-I) indicated that a large change in the d.c. ground currents occurs when two poles of the bipoles 1 and 2 are in the parallel mode of operation and the parallel modes get blocked at Dorsey first. Lines G1A, G2A and G8P experience large offset phase currents whose waveshapes are similar to that of the d.c. ground current. The offset phase currents cause a high neutral or residual current to flow in the neutral over current relay on each of these lines.

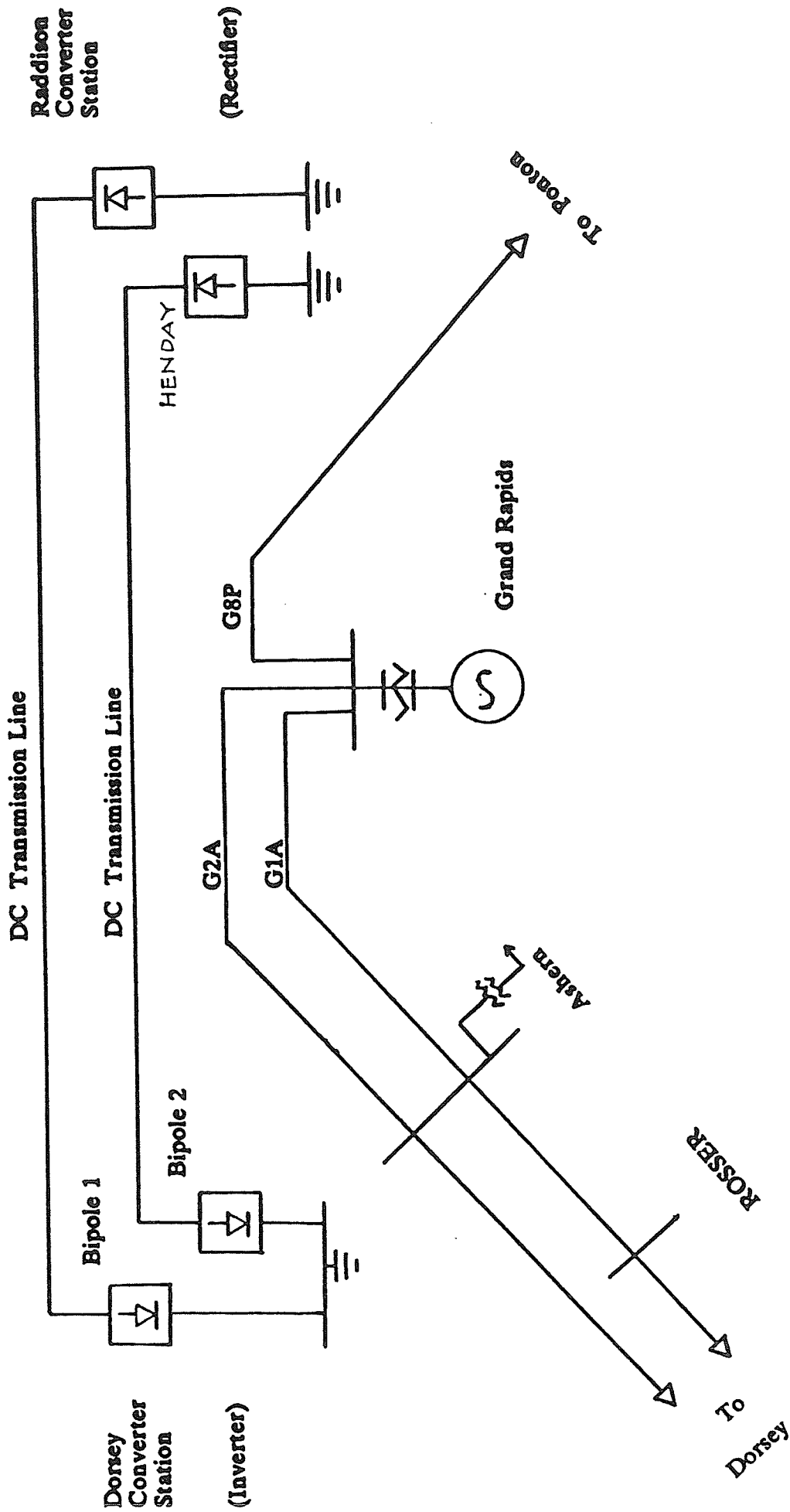


Fig. 1.1 A Single Line Diagram of the System and the concerned lines at the time of parallel operation test.

The actual recorded waveforms are also shown in Figs. 2 and 3 of Appendix-I. These should be compared with the results of Chapter 4.

Different explanations and theories were suggested about the cause of tripping of the ac lines but no final conclusions were reached. Then in consultation with the University of Manitoba, it was decided to study the phenomenon involved on a simple multiconductor system separately.

Purpose

The purpose of this thesis is to develop a model for a multiconductor system with an aim to study the cause of zero sequence currents found in a nearby ac line due to transients in dc line with ground return path. How do these induced currents vary with the change in different parameters involved such as frequency, ground resistivity, distance between the ac and dc lines. The model is to be developed with an intention of extending it to any number of conductors and ground wires later on.

Method

A literature survey was carried out which yielded some indirect piecemeal work done in this area. Much of the original work related to ground return problems of transmission lines was carried out during the 1920's and 1930's. One of the most important contributions was made by Carson in 1926^[1] when he worked out an earth correction term for calculating self and mutual impedances of the lines. Later on some useful mathematical techniques and approximations were developed to deal with the complex formulae required to

analyze the transmission line problems.

To study the present problem, a simplified system consisting of two conductors was taken as shown in Fig (2.2). Line #1 is assumed to be a dc line with a current source at the sending end while the other is an ac line. The ac line has been grounded at both ends. The inductance termination of the ac line represents the zero sequence impedance of the terminal transformers because we are only interested in the zero sequence behavior, i.e., in the part of the current that enters the ground. In reality, the normal positive and negative sequence currents are superposed on the zero sequence solution obtained here.

A general digital simulation program was developed to simulate this simple system. Chapters 2 and 3 provide the theory used in developing the model. Chapter 2 presents the method of calculating the basic matrices known as the impedance matrix and the admittance matrix. In chapter 3, the solution to the differential equations governing the voltages and currents along the transmission line is given. Two port theory is also discussed briefly to represent the transmission line as a two port network. Once the desired model was completed, a short circuit test explained in chapter 4 was conducted on it to check its validity.

After ensuring the proper working of the model, a number of runs of the program were carried out with different parameters changing such as ground resistivity, frequency etc. Interesting results were recorded. It was found that a strong coupling exists between the adjacent lines 1 and 2 at lower frequen-

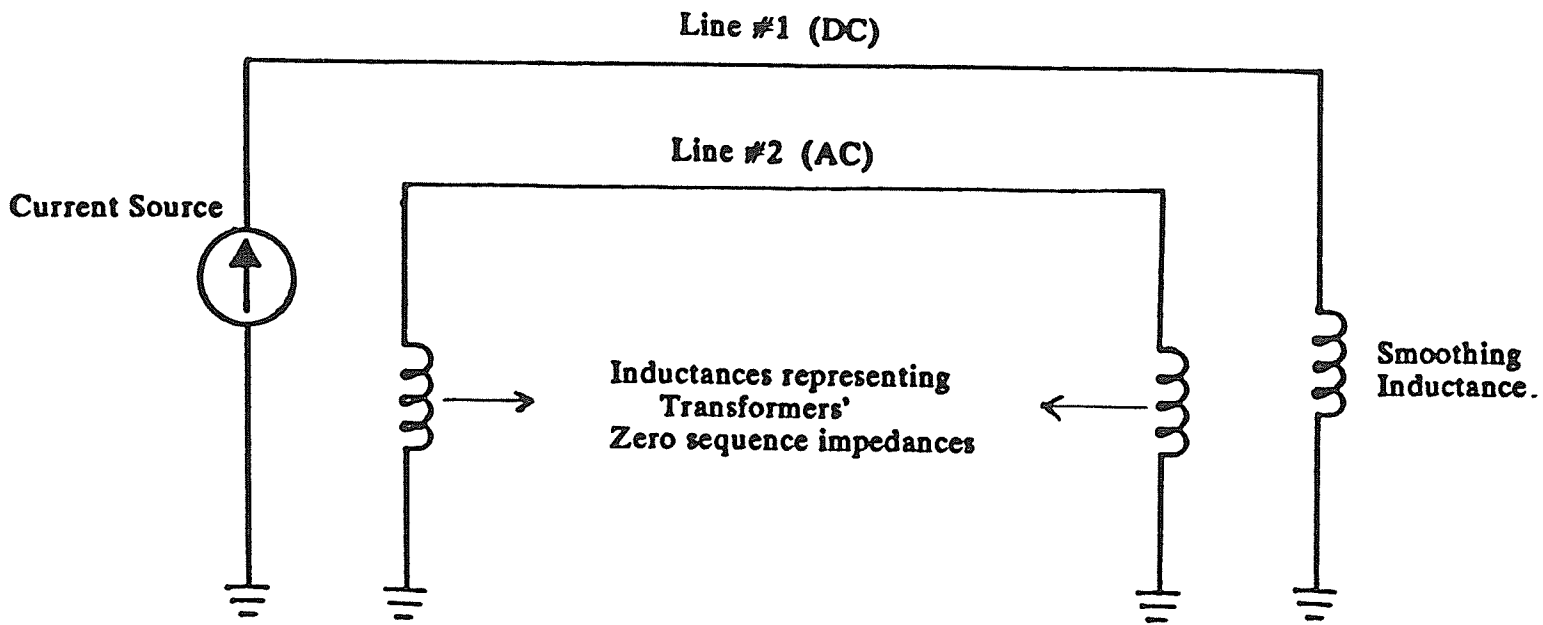


Fig 12 A simple two-conductor system with ground return.

cies even if the lines are considerably apart. This depends upon how deep the current flows into the ground. This is a function of transient currents' frequency and the resistivity of the ground. It is a well known fact of electromagnetic theory that high frequency current in a conductor tends to flow near the skin of the conductor. As the frequency is reduced, the current flows more evenly over the wire cross section. Thus, the "depth of penetration" of the current in the conductor diminishes with increasing frequency. As long as this depth of penetration of the current into the ground is large as compared to the distance between the lines, there is electromagnetic coupling between the lines. It was also observed that the inclusion of a ground wire with the ac line does not have any appreciable effect on the induced current in it. A standard fast fourier transform program was also included to obtain the coupled current waveforms to a general (non sinusoidal) input current.

Scope

A simple multiconductor model is developed to study the induction effects between the lines with ground return path. This provides a sufficiently simple system to do a parametric study of zero sequence current induction. It could subsequently be extended to a detailed model of a big system with several ground return paths. The model can also analyze the effects of ground wires present in the system. It can handle any type of input current waveforms.

CHAPTER 2

LINE PARAMETER CALCULATIONS OF A MULTICONDUCTOR SYSTEM

2.1 General

In order to model the transmission line it is necessary to obtain its electrical parameters (inductance and capacitance) from its geometrical layout and resistivity of the ground along its right of way. In this section, the basic matrices of the conductor system are presented taking into account the effects of conductor geometry, conductor internal impedance, earth return path etc. A multiconductor line is defined by its series impedance matrix Z per unit length and its shunt admittance matrix Y per unit length. It involves a number of complex mathematical expressions if one wants to calculate them in their totality. Different authors have tried and succeeded in developing somewhat simpler alternative formulas/approximations for one or more of the expressions involved in the calculation of line parameters. A survey was carried out in this regard. Efforts were made to put together these alternative expressions/approximations in order to make overall calculation of the basic matrices simpler and less time consuming without sacrificing the accuracy over a considerable range of frequencies with respect to power system operations.

2.2 Transmission Line Differential Equations

The differential equations describing electromagnetic waves along a multiconductor transmission system of n conductors are:

$$-\frac{\partial [v]}{\partial x} = [L] \frac{\partial [i]}{\partial t} + [R] [i] \quad (2.1)$$

$$-\frac{\partial [i]}{\partial x} = [C] \frac{\partial [v]}{\partial t} + [G] [v] \quad (2.2)$$

where $[v]$ and $[i]$ are column matrices (of order $n \times 1$) of voltage and current respectively, and $[L]$, $[R]$, $[C]$ and $[G]$ are square matrices (of order $n \times n$), defining inductance, resistance, capacitance and conductance respectively.

Transforming equations (2.1) and (2.2) to phasors produces equations as a function of frequency as follows

$$-\frac{d[V]}{dx} = [Z(\omega)] [I] \quad (2.3)$$

$$-\frac{d[I]}{dx} = [Y(\omega)] [V] \quad (2.4)$$

where

$$[Z(\omega)] = [R(\omega)] + j(\omega) [L(\omega)]$$

$$[Y(\omega)] = [G(\omega)] + j(\omega) [C(\omega)]$$

Therefore, in frequency domain the equations (2.3) and (2.4) can simply be written as (omitting matrix brackets for convenience)

$$\frac{dV}{dx} = -ZI \quad (2.5)$$

$$\frac{dI}{dx} = -YV \quad (2.6)$$

where

$$Z = R + j\omega L \quad (2.7)$$

$$Y = G + j\omega C \quad (2.8)$$

The solution of equations (2.5) and (2.6) shall give the propagation of voltage and current along a multiconductor system.

2.3 Modelling of a Simple Multiconductor System with Ground Return

To study the phenomenon involved in the main problem, a simple two conductor system is taken as shown in fig. (2.1). From this point onward, all the theory presented in chapters 2 and 3 shall be related to this system from time to time. In chapter 4, this system will be simulated in detail to observe the induction effects between the two lines at low frequencies with the different parameters changing. Line #1 is considered to be a dc line with ground return and a current source at its sending end. Line #2 is assumed to be an ac line with ground return and no source of current in it. The inductances at the end of line 2 represent the zero sequence impedance of transformers where the ac line terminates. The input data used in the analysis of this system is tabulated in Table (2.1).

The equations (2.5) and (2.6) for this particular system will become

$$\frac{d}{dx} \begin{bmatrix} V_1 \\ V_2 \end{bmatrix} = - \begin{bmatrix} z_{11} & z_{12} \\ z_{21} & z_{22} \end{bmatrix} \begin{bmatrix} I_1 \\ I_2 \end{bmatrix} \quad (2.9)$$

and

$$\frac{d}{dx} \begin{bmatrix} I_1 \\ I_2 \end{bmatrix} = - \begin{bmatrix} y_{11} & y_{12} \\ y_{21} & y_{22} \end{bmatrix} \begin{bmatrix} V_1 \\ V_2 \end{bmatrix} \quad (2.10)$$

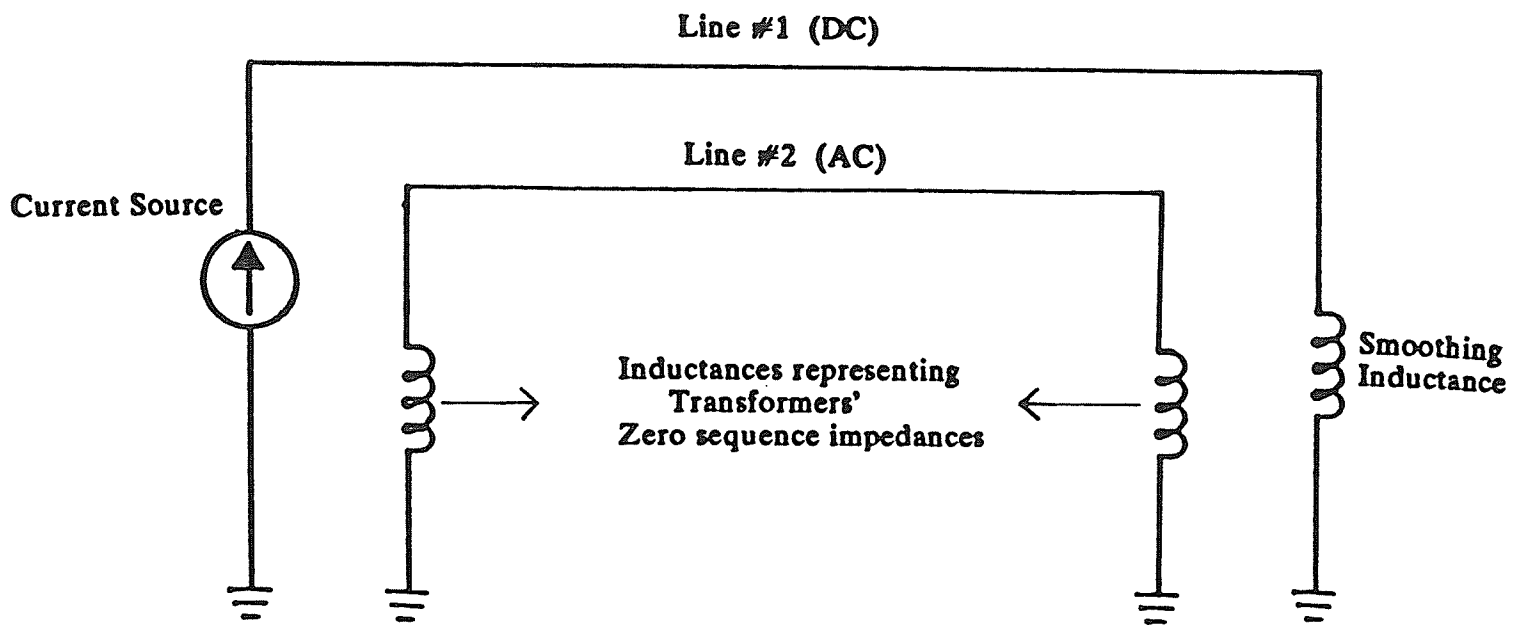


Fig. 2.1 A two-conductor system with ground return.

Table 2-1 Input data describing the system shown in fig (2.1)				
S. no	Description	Quantity	Units	Remarks
1	Number of Conductors	2	nos	
2	Type of Conductor 1	-	-	Aluminum bundled conductor having 2 conductors in it
3	Type of Conductor 2	-	-	-do-
4	Actual radius of each conductor in the bundle (a) Conductor 1 (r_1) (b) Conductor 2 (r_2)	0.02032 0.0254	metres metres	
5	Geometric mean radius of (a) Conductor 1 (GMR_1) (b) Conductor 2 (GMR_2)	0.0681554 0.1077631	metres metres	
6	Resistivity of (a) Conductor 1 (ρ_1) (b) Conductor 2 (ρ_2)	0.28248×10^{-7} 0.28248×10^{-7}	ohm-metre ohm-metre	
7	Spacing between conductors 1 and 2 (S)	182.88	metres	
8	Height above the ground of (a) Conductor 1 (h_1) (b) Conductor 2 (h_2)	18.288 14.0208	metres metres	
9	Ground Resistivity (ρ)	100	ohm-metre	
10	Frequency (f)	10	hz	
11	Current injected at sending end of line 1 (I_1)	1	ampere	
12	Terminating inductances (a) L_2 (Transformer) (b) L_3 (Smoothing) (c) L_4 (Transformer)	0.0702 0.5 0.0702	henry henry henry	
13	The permeability of free space (μ_0)	$4\pi \times 10^{-7}$	henry per metre	
14	The permittivity of free space (ϵ_0)	8.85×10^{-12}	farads per metre	

where

V_1, I_1, V_2, I_2 - the voltages and currents at point x along the conductors 1 and 2 respectively.

$z_{11}, y_{11}, z_{22}, y_{22}$ - the self impedances and admittances of conductors 1 and 2 respectively.

$z_{12}, y_{12}, z_{21}, y_{21}$ - the mutual impedance and admittances between conductors 1 and 2 respectively.

Before equations (2.9) and (2.10) are solved for V 's and I 's, it is necessary to find the impedance matrix and the admittance matrix commonly known as the Z -matrix and the Y -matrix.

2.4 Calculation of Impedance Matrix (Z -matrix)

Ignoring the proximity effect between adjacent conductors (i.e. non symmetric flow of current in conductor's cross section caused by adjacent conductors), and conductors and ground, the elements of the Z -matrix may be divided into two categories as follows

- (i) elements representing the self impedance of the conductor, say i . (z_{ii})
- (ii) elements representing the mutual impedance between the conductor i and the conductor j . (z_{ij})

These elements of the Z -matrix can be calculated using the relations presented next.

2.4.1 Calculation of Self-Impedance

The self impedance of the conductor may be regarded as made up of the following two components.

- (a) the internal impedance of the conductor or $(z_{ii})_{INT}$
- (b) the external impedance of the conductor or $(z_{ii})_{EXT}$

Thus

$$z_{ii} \text{ (or } z_{self} \text{)} = (z_{ii})_{INT} + (z_{ii})_{EXT} \quad (2.9)$$

(a) Calculation of Internal Impedance $(z_{ii})_{INT}$

When current flows in a conductor, it produces a magnetic field around it. Some of the magnetic field is due to the flux inside the conductor. The changing lines of flux inside the conductor also contribute to the induced voltage in a circuit and therefore to the inductance. Since impedance consists of resistance and inductive reactance, at low frequencies, $(z_{ii})_{INT}$ is equal to the dc resistance of the conductor. At higher frequencies, it is given by the classical formula^[2]

$$(z_{ii})_{INT} = \frac{\rho_i m I_0(mr_i)}{2\pi r_i I_1(mr_i)} \quad \text{ohm/metre} \quad (2.10)$$

where

$$m = \sqrt{\frac{j\omega\mu}{\rho_i}} \quad (2.11)$$

and I_0, I_1 are the modified Bessel functions of order 0.

An approximation to the above formula is found in a paper^[4] which has made the calculations much easier without using Bessel functions. The inter-

nal impedance of a circular conductor can be calculated to a reasonable accuracy by using the following expression.

$$(z_{ii})_{INT} = \left(\frac{\rho_i m}{2\pi r_i} \coth(0.777 m r_i) + \frac{0.3565 \rho_i}{\pi r_i^2} \right) \text{ ohm /metre} \quad (2.12)$$

An error analysis done by the authors shows that there can be maximum error of 4% in the real (resistive) part of equation (2.12) when $|mr_i| = 5$, whereas the maximum error in reactive (imaginary) part of (2.12) is 5% when $|mr_i| = 3.5$. Apart from these maxima the formula is quite accurate. Moreover, it is justified by the fact that this expression requires less digital computation than that of (2.10) to which this is an approximation.

(b) Calculation of External Impedance $(z_{ii})_{EXT}$

Since the resistance is a quantity entirely 'internal' to the conductor, the external impedance will be nothing but the inductive component due to external flux linkages of the conductor. It is dependent upon the properties of the medium filling the interconductor space. Since we are interested in conductors carrying current with ground as return path, the medium filling the interconductor space will be air and the ground. The Fig. (2.2) shows two such separate conductors i and j respectively. The usual method of finding inductance of the lines with ground return is by considering the images of the conductors as shown in Fig. (2.2). Had the ground been a perfect conductor, a conductor's image will be exactly at the same depth as it is above the ground. In such a case an equal and opposite field will be produced by the conductor and its image respectively. Therefore there will not be any inductive com-

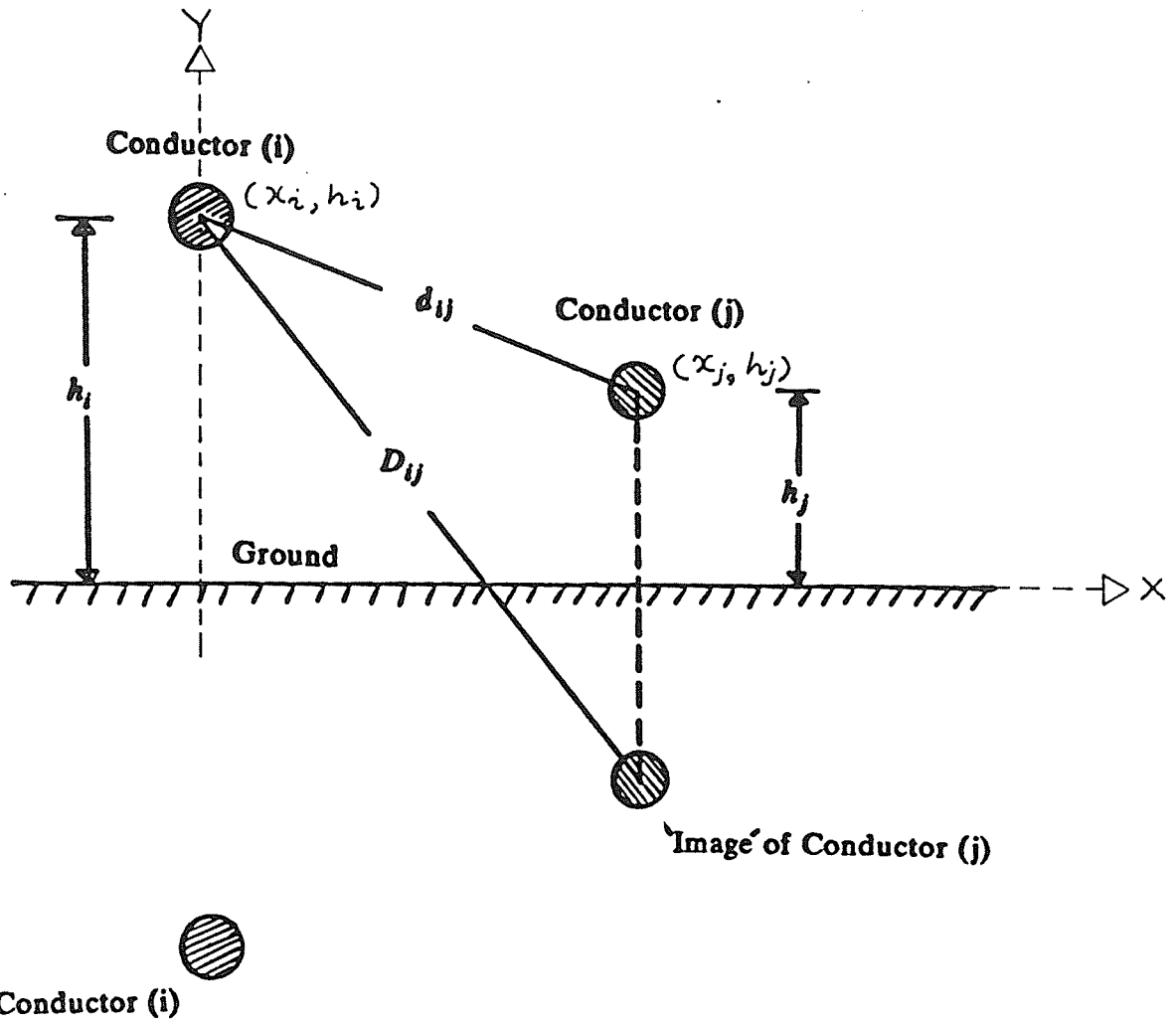


Fig. 2.2 Physical geometry of the conductors i and j.

ponent due to the ground medium. But unfortunately this is not the case in real life. Ground is not a perfect conductor and therefore the image of conductor cannot be at the same depth as the height of the conductor above the ground. In other words the depth of penetration of current is not same for all the cases but depends upon the ground conductivity etc. In 1926, J. R. Carson^[1] worked out an earth correction term which gives the additional reactance due to the ground. He found that the depth of penetration of current into the ground is a function of frequency and the ground resistivity.

Carson derived the following expression for calculating the self external impedance of conductor i ,^[6]

$$(z_{ii})_{EXT} = j\omega \frac{\mu_0}{2\pi} \ln \frac{2h}{r_i} + \omega \frac{\mu}{\pi} J_i \quad ; \mu = \mu_0 \quad (2.13)$$

where the ground correction term J_i is infinite integral and is given by

$$J_i = P + jQ = \int_0^{\infty} \frac{j e^{-2hi\lambda}}{\lambda + \sqrt{\lambda^2 + j\omega\mu}} d\lambda \quad (2.14)$$

The only hard part of Carson's earth correction term is the evaluation of infinite integral with complex arguments. Later on some approximations to this were suggested by different authors but most of them are valid over a limited range of frequency. In 1981, A. Deri of Technical University of Budapest and A. Semlyen of University of Toronto^[6] provided a simple but an accurate substitute to the equation (2.13) over the whole range of frequencies for which Carson's derivation is valid.

The Deri-Semlyen paper^[6] derived the following approximation to the Carson's equation (2.13) for calculating the external impedance of the conductor *i*. Referring to Fig. (2.2),

$$(z_{ii})_{EXT} = j\omega \frac{\mu_0}{2\pi} \ln \frac{2h_i}{r_i} + j\omega \frac{\mu_0}{2\pi} \ln \left(\frac{2(h_i + de)}{2h_i} \right) \quad \text{ohm / metre} \quad (2.15)$$

$$= \frac{j\omega\mu_0}{2\pi} \ln \left(\frac{2h_i + de}{r_i} \right) \quad (2.16)$$

where

r_i = radius of conductor *i*

h_i = height of the conductor *i* above the ground

de = depth of penetration of current into the ground

$$= \sqrt{\frac{\rho}{j\omega\mu_0}} \quad (2.17)$$

ρ = ground resistivity

(Note: For a bundled conductor, r_i will be replaced by the GMR i.e. geometric mean radius of the bundled conductor).

Thus, the self impedance of a multiconductor system or the z_{ii} elements of the Z-matrix will be given by substituting equations (2.12) and (2.16) in (2.9), i.e.

$$z_{ii} = \left(\frac{\rho_i m}{2\pi r_i} \coth(0.777mr_i) + \frac{0.3565\rho_i}{\pi r_i^2} \right) + \left(\frac{j\omega\mu_0}{2\pi} \ln \left(\frac{2(h_i + de)}{r_i} \right) \right) \quad \text{ohm / metre} \quad (2.18)$$

where

$$de = \sqrt{\frac{\rho}{j\omega\mu}} \quad (2.19)$$

and

$$m = \sqrt{\frac{j \omega \mu}{\rho_i}} \quad (2.20)$$

The main feature of the above equation is that all the diagonal elements of the Z-matrix can be calculated by hand held calculators for a particular frequency and ground resistivity.

Now substituting the data provided in Table (2-1) for the system of Fig. (2.1) in equation (2-17), the self impedance at a frequency of 10 Hz is calculated as

$$z_{11} = 0.2069 \times 10^{-4} + j 0.1325 \times 10^{-3} \quad \text{ohm / metre} \quad (2.21)$$

and

$$z_{22} = 0.1685 \times 10^{-4} + j 0.1267 \times 10^{-3} \quad \text{ohm / metre} \quad (2.22)$$

(The 10 Hz value is only as an example to demonstrate the calculations procedure. Also, it is the major frequency present in the actual time domain signal)

2.4.2 Calculation of Mutual Impedances (z_{ij})

Mutual impedance is nothing but the mutual reactance between the two conductors or circuits and is the result of flux linkages of one conductor or circuit due to the current in the second conductor or circuit. As in the case of calculation of external impedance, it is also dependent upon the medium filling the interconductor space. Again, for conductors shown in Fig. (2.2), Carson derived the following expression^[1] for calculating the mutual impedance (or reactance) between the conductor i and the conductor j.

$$z_{ij} = \frac{j\omega\mu_0}{2\pi} \ln \frac{\sqrt{(h_i+h_j)^2 + (x_i-x_j)^2}}{\sqrt{(h_i-h_j)^2 + (x_i-x_j)^2}} + \frac{\omega\mu_0}{\pi} J_m \quad (2.23)$$

where

$$J_m = P_m + j Q_m = \int_0^{\infty} \frac{je^{-(h_i+h_j)\lambda}}{\lambda + \sqrt{\lambda^2 + j\omega\mu_0}} \cos \lambda(x_i-x_j) d\lambda \quad (2.24)$$

This infinite integral with complex arguments is difficult to evaluate numerically but the Deri-Semlyen paper^[6] gives a very simple and an accurate approximation to the equation (2.23). With reference to Fig.(2.2), they developed the following expression for calculating the mutual impedance between the conductors i and j with ground return path.

$$z_{ij} = \frac{j\omega\mu_0}{2\pi} \ln \frac{\sqrt{(x_i-x_j)^2 + (y_i+y_j+2de)^2}}{\sqrt{(x_i-x_j)^2 + (y_i-y_j)^2}} \quad \text{ohm / metre} \quad (2.25)$$

where

de = depth of penetration of current into the ground (metres)

$$= \sqrt{\frac{\rho}{j\omega\mu}}$$

ρ = ground resistivity

This value of z_{ij} exactly equals the asymptotic expansions of Carson's integral at extremely low and high frequencies with acceptable error in between.

Equation (2.25) gives us a fairly simple expression for calculating the off-diagonal elements of the Z-matrix.

Thus with the help of equations (2.18) and (2.25), the complete Z-matrix can be calculated for the parameters given in Table 2-1.

Now substituting the values from Table (2-1) in equation (2.25), the

mutual impedance for our system will be

$$z_{12} = z_{21} = j \frac{2\pi \times 60 \times 4\pi \times 10^{-7}}{2\pi} \ln \frac{\sqrt{(0-182.88)^2 + (18.288+14.02+de)^2}}{\sqrt{(0-182.88)^2 + (18.288-14.02)^2}}$$

where

$$de = \sqrt{\frac{100}{j 2\pi \times 60 \times 4\pi \times 10^{-7}}}$$

$$= 795.7747 - j 795.7747 \text{ metres}$$

or

$$z_{12} = z_{21} = 0.9703 \times 10^{-5} + j 0.3167 \times 10^{-4} \text{ ohms /metre} \quad (2.26)$$

Thus by combining equations (2.21), (2.22) and (2.26), we get

$$Z = \begin{bmatrix} 0.2069 \times 10^{-4} + j 0.1325 \times 10^{-3} & 0.9703 \times 10^{-5} + j 0.3167 \times 10^{-4} \\ 0.9703 \times 10^{-5} + j 0.3167 \times 10^{-4} & 0.1685 \times 10^{-4} + j 0.1267 \times 10^{-3} \end{bmatrix} \quad (2.27)$$

2.5 Calculation of the Admittance Matrix (Y-Matrix)

The admittance of a conductor comprises of the distributed capacitance and the distributed conductance G. These parameters are entirely 'external' quantities i.e. totally independent of the material of the conductors or of the transverse extension of the conductors on either side of the interconductor space. They are functions only of the nature and dimensions of the material filling the interconductor space, and of the frequency. Thus the admittance matrix Y is a only a function of physical geometry of the conductors relative to the earth plane, because the conductor and the earth surfaces may each be regarded as equipotential surfaces.

The Y-matrix is assumed to have no real part because the conductance of the air is negligible. The elements of the Y-matrix with respect to Fig. (2.2) are given by^[5]

$$Y = \left[j 2\pi \omega \epsilon_0 \left(\ln \frac{D_{ij}}{d_{ij}} \right) \right]^{-1}, i = 1(1)n, j = 1(1)n \quad (2.28)$$

where

D_{ij} = distance between conductor i and conductor j

$$= \sqrt{(x_i - x_j)^2 + (y_i + y_j)^2} \quad (2.29)$$

$$D_{ii} = 2h_i \quad (2.30)$$

$$D_{jj} = 2h_j \quad (2.31)$$

$$= \sqrt{(x_i - x_j)^2 + (y_i - y_j)^2} \quad (2.32)$$

$$d_{ii} = \text{radius of the conductor } i \quad (2.33)$$

$$d_{jj} = \text{radius of the conductor } j \quad (2.34)$$

In case of 2x2 conductor system, the equation (2.28) produces the Y-matrix as follows

$$Y = j 2\pi \omega \epsilon_0 \begin{bmatrix} \ln \frac{D_{11}}{d_{11}} & \ln \frac{D_{12}}{d_{12}} \\ \ln \frac{D_{21}}{d_{21}} & \ln \frac{D_{22}}{d_{22}} \end{bmatrix}^{-1} \quad (2.35)$$

Now using the data given in Table (2-1) in equations (2.29) to (2.34) we can calculate

$$D_{12} = D_{21} = \sqrt{(0-182.88)^2 + (18.288+14.025)^2}$$

($x_1 = 0$, because conductor 1 is taken as reference with respect to conductor 2)

$$D_{11} = 2 \times 18.2880 = 36.5760 \text{ metres}$$

$$D_{22} = 2 \times 14.0208 = 28.0416 \text{ metres}$$

$$d_{12} = d_{21} = \sqrt{(0-182.88)^2 + (18.288-14.025)^2} = 182.9298 \text{ metres}$$

$$d_{11} = 0.0681544 \text{ metres}$$

$$d_{22} = 0.1077631 \text{ metres}$$

$$2\pi \omega \epsilon_0 = 2\pi \times 2\pi \times 60 \times 8.85 \times 10^{-12} = 3.4938 \times 10^{-9}$$

Substituting the respective values in equation (2.35) leads to

$$Y = j \begin{bmatrix} 0.5559 \times 10^{-9} & -0.1509 \times 10^{-11} \\ -0.1509 \times 10^{-11} & 0.6282 \times 10^{-9} \end{bmatrix} \quad (2.36)$$

2.6 Elimination of Ground Wires

Consider a simple two conductor system, each conductor carrying a ground wire alongwith it. With this system in hand, one will end up with a 4x4 Z-matrix and a 4x4 Y-matrix since now there are four conductors in all. All the further analysis of solving transmission line differential equations will involve these 4x4 matrices. But with a little manipulation, the order of these basic matrices can again be reduced to the order equal to the number of non grounded conductors (i.e. 2x2 in the above example), and at the same time, the effect of ground wires will be taken into account. This will help in making the overall computations of solving a multiconductor system having ground wires, simpler and less time consuming. The technique of eliminating ground wires while considering their effect is briefly examined here.

Rewriting the transmission line differential equations (2.5) and (2.6),

$$\frac{dV}{dX} = -ZI \quad (2.37)$$

$$\frac{dI}{dX} = -YV \quad (2.38)$$

Let us assume that the impedance matrix Z and the admittance matrix Y in the above equation take into account the ground conductors also.

The partitioning of the matrix equation (2.37) with respect to ground voltage, ground current and ground conductors gives

$$\frac{d}{dx} \begin{bmatrix} V_c \\ V_g \end{bmatrix} = - \begin{bmatrix} z_{cc} & z_{cg} \\ z_{gc} & z_{gg} \end{bmatrix} \begin{bmatrix} I_c \\ I_g \end{bmatrix} \quad (2.39)$$

where the suffix c is meant for non grounded conductors, while the suffix g is for grounded conductors.

The above equation (2.39) can easily be understood if it is written for a 2x2 conductor system with one ground wire. Let there be conductor 1 without ground wire and conductor 2 with ground wire marked as conductor 3. For this simple system, the equation (2.39) will become

$$\frac{d}{dx} \begin{bmatrix} V_1 \\ V_2 \\ V_3(=V_g) \end{bmatrix} = - \begin{bmatrix} z_{11} & z_{12} & z_{13} \\ z_{21} & z_{22} & z_{23} \\ z_{31} & z_{32} & z_{33} \end{bmatrix} \begin{bmatrix} I_1 \\ I_2 \\ I_3(=I_g) \end{bmatrix} \quad (2.40)$$

Now in most of the cases the ground wires are earthed at every tower. It is valid to assume that ground wire potential is zero everywhere at normal frequencies (upto 300 khz) i.e. $V_g = 0$

Using this, equation (2.39) can be written as follows

$$\frac{dV_c}{dx} = -z_{cc} I_c - z_{cg} I_g \quad (2.41)$$

$$0 = -z_{gc} I_c - z_{gg} I_g \quad (2.42)$$

Eliminating I_g from the above pair of equations to obtain

$$\frac{dV_c}{dx} = -Z^1 I_c \quad (2.43)$$

where

Z^1 = the reduced impedance matrix of the order equal to number of non grounded conductors

$$= z_{cc} - z_{cg} z_{gg}^{-1} z_{gc} \quad (2.44)$$

Similarly the Y matrix can also be reduced. For this the equation (2.38) can be partitioned as before to give

$$\frac{d}{dx} \begin{bmatrix} I_c \\ I_g \end{bmatrix} = - \begin{bmatrix} y_{cc} & y_{cg} \\ y_{gc} & y_{gg} \end{bmatrix} \begin{bmatrix} V_c \\ V_g \end{bmatrix} \quad (2.45)$$

Since $V_g = 0$, equation (2.45) can be reduced to

$$\frac{dI_c}{dx} = -Y^1 V_c \quad (2.46)$$

where

$$Y^1 = y_{cc} \quad (2.47)$$

= the reduced admittance matrix of the order equal to number of non grounded conductors.

Thus the impedance matrix Z^1 and the admittance matrix Y^1 in differential equations (2.43) and (2.46) respectively are of the order equal to number of non grounded conductors but at the same time carrying the ground wires effect in them.

CHAPTER 3
SOLUTION
TO
TRANSMISSION LINE DIFFERENTIAL EQUATIONS
OF
A MULTICONDUCTOR SYSTEM

3.1 Introduction

In the previous chapter, the differential equations governing voltage and current distribution along the transmission lines of a multiconductor system were presented. So far only the Z- matrix and the Y-matrix involved in these were described and calculated. After the calculation of these matrices, the next step is to solve those differential equations so as to enable us to find out the voltage and current at any point along the lines in a multiconductor system. Efforts are being made to present the solution in its simplest form. At the end of the chapter, two-port theory of representing transmission lines is briefly discussed as the same will be used in Chapter 4 for analyzing our model.

3.2 Solution to Transmission Line Differential Equations of a Multiconductor System

Restating the differential equations (2.5) and (2.6) from the last chapter, which describe the voltage and current at a point along the transmission lines

of a multiconductor system, comprising of n conductors,

$$\frac{dV}{dx} = -ZI \quad (3.1)$$

$$\frac{dI}{dx} = -YV \quad (3.2)$$

where V and I are column matrices (of order $n \times 1$) of voltage and current, and Z and Y are the square matrices (of order $n \times n$) defining line parameters.

The method to solve the above mentioned differential equations is presented below.

Eliminating either V or I from equations (3.1) and (3.2) respectively, one obtains

$$\frac{d^2V}{dx^2} = -Z \frac{dI}{dx} = ZYV \quad (3.3)$$

$$\frac{d^2I}{dx^2} = -Y \frac{dV}{dx} = YZI \quad (3.4)$$

The solutions of equations (3.3) and (3.4) for V and I respectively, must be expressions which when differentiated twice with respect to x obtain the original expression multiplied by ZY . For example, the solution for V when differentiated twice with respect to x must yield ZYV . This suggests an exponential form of the solution. Let us first solve equation (3.3) for V and then equation (3.4) for I .

3.2.1 Propagation of Voltage

Assume the solution of equation (3.3) is of the following form

$$V_x = e^{-\gamma x} V_A + e^{\gamma x} V_B \quad (3.5)$$

where γ is referred to as a propagation constant matrix and will be evaluated

shortly, and V_A, V_B are column matrices (nx1) representing constants of integration to be determined from the boundary conditions.

Now

$$\frac{d}{dx}(e^{-\gamma x}) = -\gamma e^{-\gamma x} \quad (3.6)$$

and

$$\frac{d}{dx}(e^{\gamma x}) = \gamma e^{\gamma x} \quad (3.7)$$

Using (3.6) and (3.7), the second derivative of V_x from equation (3.5) with respect to x produces

$$\frac{d^2 V_x}{dx^2} = \gamma^2 V \quad (3.8)$$

Comparison of equations (3.3) and (3.8) gives

$$\gamma^2 V = ZYV$$

or

$$\gamma^2 = ZY$$

or

$$\gamma = [ZY]^{1/2} \quad (3.9)$$

Thus the voltage propagation constant is equal to the square root of the multiplication of the impedance matrix and the admittance matrix. Note that the propagation constant is a complex quantity in which the real part is known as attenuation constant α while the imaginary part is called the phase constant β . The properties of $e^{\pm \gamma x}$ or $e^{\pm (\alpha + j\beta)x}$ in equation (3.5) help to explain the vari-

ation of the phasor values of voltage as a function of distance along the line.

Now let

$$A = ZY = Z_1 Y_1 = (YZ)_1$$

Therefore, the propagation constant is given by

$$\gamma = \sqrt{A} \quad (3.10)$$

To solve the equation (3.5) for V_x , $\gamma(=\sqrt{A})$ and $e^{\pm \gamma x}$ are to be evaluated, remembering A is a complex square matrix of order n . This could have proved tedious to work out but some linear algebra techniques have made this job considerably easy. The aim is to diagonalize the matrix A so that the desired mathematical/ trigonometric operations could be performed easily. This can be achieved with the help of eigenvector algebra. The method of finding eigenvectors and eigenvalues of a matrix is assumed to be known here^[13]. Once the eigenvalues and eigenvectors of a matrix are known it becomes easy to diagonalize the same matrix as shall be shown below.

Let λ be the square diagonal matrix of order n , as follows

$$\lambda = \begin{bmatrix} \lambda_1 & 0 & 0 & \cdot & 0 \\ 0 & \lambda_2 & 0 & \cdot & 0 \\ \cdot & \cdot & \cdot & \cdot & \cdot \\ \cdot & \cdot & \cdot & \cdot & \cdot \\ 0 & 0 & 0 & \cdot & \lambda_0 \end{bmatrix} \quad (3.11)$$

where $\lambda_1, \lambda_2, \dots, \lambda_n$ are the distinct eigenvalues of A . Let E_v be the square matrix of order n , the columns of which represent the eigenvectors corresponding to their respective eigenvalues. i.e.

$$E_v = \begin{bmatrix} E_{v_1} & E_{v_2} & E_{v_3} & \dots & \dots & E_{v_n} \\ \cdot & \cdot & \cdot & \cdot & \cdot & \cdot \\ \cdot & \cdot & \cdot & \cdot & \cdot & \cdot \\ \cdot & \cdot & \cdot & \cdot & \cdot & \cdot \\ \cdot & \cdot & \cdot & \cdot & \cdot & \cdot \end{bmatrix} \quad (3.12)$$

where $E_{v_1}, E_{v_2}, \dots, E_{v_n}$ are the eigenvectors of the matrix A corresponding to its eigenvalues $\lambda_1, \lambda_2, \dots, \lambda_n$ respectively.

Now A can be diagonalized by simply performing the following operations

$$E_v^{-1} A E_v = \lambda \quad (3.13)$$

(Note: the proof of the above relation can be found in any book on linear algebra)

or

$$E_v^{-1} \sqrt{A} E_v = \sqrt{\lambda}$$

or

$$\sqrt{A} = E_v \sqrt{\lambda} E_v^{-1} \quad (3.14)$$

Note that the right hand expression is simple to solve as the square root of λ is nothing but the square root of its respective diagonal elements. Thus \sqrt{A} can be found easily and hence the propagation constant γ i.e.

$$\gamma = \sqrt{A} = E_v \sqrt{\lambda} E_v^{-1} \quad (3.15)$$

To find $e^{\pm \gamma x}$, rearrange the equation (3.13) to get

$$E_v^{-1} \gamma E_v = \sqrt{\lambda}, \text{ still a diagonal matrix.}$$

or

$$E_v^{-1} e^{\pm \gamma x} E_v = e^{\pm \sqrt{\lambda} x}$$

or

$$e^{\pm \gamma x} = E_v e^{\pm \sqrt{\lambda} x} E_v^{-1} \quad (3.16)$$

Substituting for $e^{\pm \gamma x}$ from equation (3.16) in equation (3.5) produces

$$V_x = E_v e^{-\sqrt{\lambda} x} E_v^{-1} V_A + E_v e^{\sqrt{\lambda} x} E_v^{-1} V_B \quad (3.17)$$

or

$$V_x = e^{-\Gamma x} V_A + e^{\Gamma x} V_B \quad (3.18)$$

where

$$\Gamma = E_v \sqrt{\lambda} E_v^{-1} \quad (3.19)$$

$$e^{\Gamma x} = E_v e^{\sqrt{\lambda} x} E_v^{-1} \quad (3.20)$$

$$e^{-\Gamma x} = E_v e^{-\sqrt{\lambda} x} E_v^{-1} \text{ and} \quad (3.21)$$

$e^{-\Gamma x} V_A$ and $e^{\Gamma x} V_B$ are known as 'reflected' and 'incident' voltage components respectively.

The constants of integration V_A and V_B can be determined from the end conditions of the system i.e. if the voltages at any two points in the system are known, V_A and V_B can easily be calculated by substituting them in equation (3.17).

Hence equation (3.5) can be completely solved for the voltage V_x at any point x along the transmission lines in a multiconductor system. As x increases — i.e. as we progress along the system from its sending end to receiving end, the incident voltage decreases in magnitude and is retarded in phase whereas opposite happens in the case of reflected component.

3.2.2 Propagation of current

The current at a point x along the line can be found by solving the equation (3.2) for I by the same procedure used in voltage propagation or directly from equation (3.1).

$$\frac{dV_x}{dx} = -Z I_x$$

or

$$I_x = -Z^{-1} \frac{dV_x}{dx}$$

Substituting for V_x from equation (3.18) to obtain

$$\begin{aligned} I_x &= -Z^{-1} \frac{d}{dx} [e^{-\Gamma x} V_A + e^{\Gamma x} V_B] \\ &= Z^{-1} \Gamma [e^{-\Gamma x} V_A - e^{\Gamma x} V_B] \end{aligned} \quad (3.22)$$

or

$$I_x = Y_0 [e^{-\Gamma x} V_A - e^{\Gamma x} V_B] \quad (3.23)$$

where

$$Y_0 = Z^{-1} \Gamma \quad (3.24)$$

or

$$Z_0 = Y_0^{-1} = \Gamma^{-1} Z \quad (3.25)$$

Once the boundary conditions are known, equation (3.22) or (3.23) can be completely solved for propagation of current. Incident current and reflected current behave in the same manner as in the case of voltage propagation.

Physical significance of Y_0/Z_0

Consider a semi infinite line i.e. the line starts at some point but ends at infinity. Therefore, in this case there will be no reflected component of either voltage or current, and the equations (3.18) and (3.23) will be reduced to

$$V_x = e^{-\Gamma x} V_A \quad (3.26)$$

$$I_x = Y_0 e^{-\Gamma x} V_A \quad (3.27)$$

respectively.

Dividing (3.27) by (3.26) to get

$$\frac{I_x}{V_x} = Y_0$$

$$\text{or } I_x = Y_0 V_x \quad (3.28)$$

The above equation shows that the incident current is related to the incident voltage through Y_0 and is independent of distance. Y_0 is known as the characteristic admittance matrix. In the same way Z_0 is known as the characteristic impedance matrix.

3.3 Multiconductor System as a Two Port Network

In network theory, a 'port' of a network is defined as any pair of terminals at which the instantaneous current into one of the terminals is equal to the instantaneous current out of the other terminal. Therefore any section of the transmission line is a two port network and can be represented as shown in fig (3.1). As per standard convention, the currents are assumed positive when they enter a node. The object of two port theory is to develop useful relationships among various choice of pairs of the four quantities (i.e. voltage

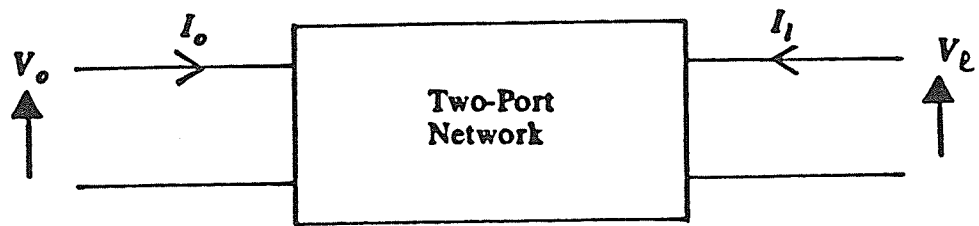


Fig. 3.1 A two-port network with the notations of the transmission line.

and current at two ports), in terms of the nature of the network. The model developed in this report has made considerable use of this theory.

To express the solution of multiconductor equations in two port theory, rewrite the equations (3.18) and (3.23)

$$V_x = e^{-\Gamma x} V_A + e^{\Gamma x} V_B \quad (3.29)$$

$$I_x = Y_0 [e^{-\Gamma x} V_A - e^{\Gamma x} V_B] \quad (3.30)$$

At $x = 0$, equations (3.29) and (3.30) become

$$V_0 = V_A + V_B \quad (3.31)$$

$$I_0 = Y_0 [V_A - V_B] \quad (3.32)$$

At $x = l$, the length of the system

$$V_l = e^{-\Gamma l} V_A + e^{\Gamma l} V_B \quad (3.33)$$

$$I_l = Y_0 [e^{-\Gamma l} V_A - e^{\Gamma l} V_B] \quad (3.34)$$

Solving (3.29) and (3.30) for V_A and V_B to obtain

$$V_A = \frac{V_0 + Z_0 I_0}{2} \quad (3.35)$$

$$V_B = \frac{V_0 - Z_0 I_0}{2} \quad (3.36)$$

where

$$Z_0 = \frac{1}{Y_0}$$

Substituting for V_A and V_B from equations (3.35) and (3.36) respectively in equation (3.33) to get

$$V_l = e^{-\Gamma l} \frac{V_0}{2} + e^{-\Gamma l} \frac{Z_0 I_0}{2} + e^{\Gamma l} \frac{V_0}{2} - e^{\Gamma l} \frac{Z_0 I_0}{2}$$

By rearranging the right hand side,

$$V_l = \frac{e^{\Gamma l} + e^{-\Gamma l}}{2} V_0 - \frac{e^{\Gamma l} - e^{-\Gamma l}}{2} Z_0 I_0$$

$$= \cosh (\Gamma l) V_0 - \sinh (\Gamma l) Z_0 I_0 \quad (3.37)$$

Similarly, we can solve (3.34) for I_l to give

$$I_l = Y_0 \sinh (\Gamma l) V_0 - Y_0 \cosh (\Gamma l) Z_0 I_0 \quad (3.38)$$

By rearranging (3.37) to obtain

$$I_0 = Y_0 \coth (\Gamma l) V_0 - Y_0 \operatorname{cosech} (\Gamma l) V_l \quad (3.39)$$

Substituting for I_0 from (3.39) in (3.38) to get

$$I_l = -Y_0 \operatorname{cosech} (\Gamma l) V_0 + Y_0 \coth (\Gamma l) V_l \quad (3.40)$$

Putting the equations (3.39) and (3.40) in matrix form

$$\begin{bmatrix} I_0 \\ I_l \end{bmatrix} = \begin{bmatrix} Y_0 \coth (\Gamma l) & -Y_0 \operatorname{cosech} (\Gamma l) \\ -Y_0 \operatorname{cosech} (\Gamma l) & Y_0 \coth (\Gamma l) \end{bmatrix} \begin{bmatrix} V_0 \\ V_l \end{bmatrix} \quad (3.41)$$

Similarly

$$\begin{bmatrix} V_0 \\ V_l \end{bmatrix} = \begin{bmatrix} Z_0 \coth (\Gamma l) & Z_0 \operatorname{cosech} (\Gamma l) \\ Z_0 \operatorname{cosech} (\Gamma l) & Z_0 \coth (\Gamma l) \end{bmatrix} \begin{bmatrix} I_0 \\ I_l \end{bmatrix} \quad (3.42)$$

Equations (3.41) and (3.42) are the multiconductor two port equations.

The system can be analyzed by observing the behavior of the elements of the matrices as the different parameters involved in the system such as frequency, physical geometry of the conductor etc. are changed. This is exactly what we will be doing in Chapter 4.

3.4 An example

Coming back to our system of fig (2.1) and treating it as a two port network as shown in fig (3.2), an attempt will be made to form a similar set of equations as those of (3.41) and (3.42).

Rewriting equations (2.27) and (2.36) from Chapter 2 to have

$$Z = \begin{bmatrix} 0.2069 \times 10^{-4} + j 0.1325 \times 10^{-3} & 0.9703 \times 10^{-5} + j 0.3167 \times 10^{-4} \\ 0.9703 \times 10^{-5} + j 0.3167 \times 10^{-4} & 0.1685 \times 10^{-4} + j 0.1267 \times 10^{-3} \end{bmatrix} \quad (3.43)$$

$$Y = \begin{bmatrix} 0.0000 + j 0.5559 \times 10^{-9} & 0.0000 - j 0.1509 \times 10^{-11} \\ 0.0000 - j 0.1509 \times 10^{-11} & 0.0000 + j 0.6282 \times 10^{-9} \end{bmatrix} \quad (3.44)$$

Now

$$A = Z Y$$

$$= \begin{bmatrix} -0.7362 \times 10^{-13} - j 0.1149 \times 10^{-13} & -0.1970 \times 10^{-13} + j 0.6064 \times 10^{-14} \\ -0.1741 \times 10^{-13} + j 0.5368 \times 10^{-14} & -0.7956 \times 10^{-13} + j 0.1057 \times 10^{-13} \end{bmatrix} \quad (3.45)$$

The eigenvalues and eigenvectors for this matrix are calculated as

$$\lambda_1 = -0.9530 \times 10^{-13} + j 0.1660 \times 10^{-13} \quad (3.46)$$

$$\lambda_2 = -0.5788 \times 10^{-13} + j 0.5453 \times 10^{-14} \quad (3.47)$$

$$E_{v_1} = \begin{bmatrix} 0.9229 - j 0.6197 \times 10^{-1} \\ 1.0 + j 0.0 \end{bmatrix} \quad (3.48)$$

$$E_{v_2} = \begin{bmatrix} 1.0 - j 0.3725 \times 10^{-8} \\ -0.8160 + j 0.5508 \times 10^{-1} \end{bmatrix} \quad (3.49)$$

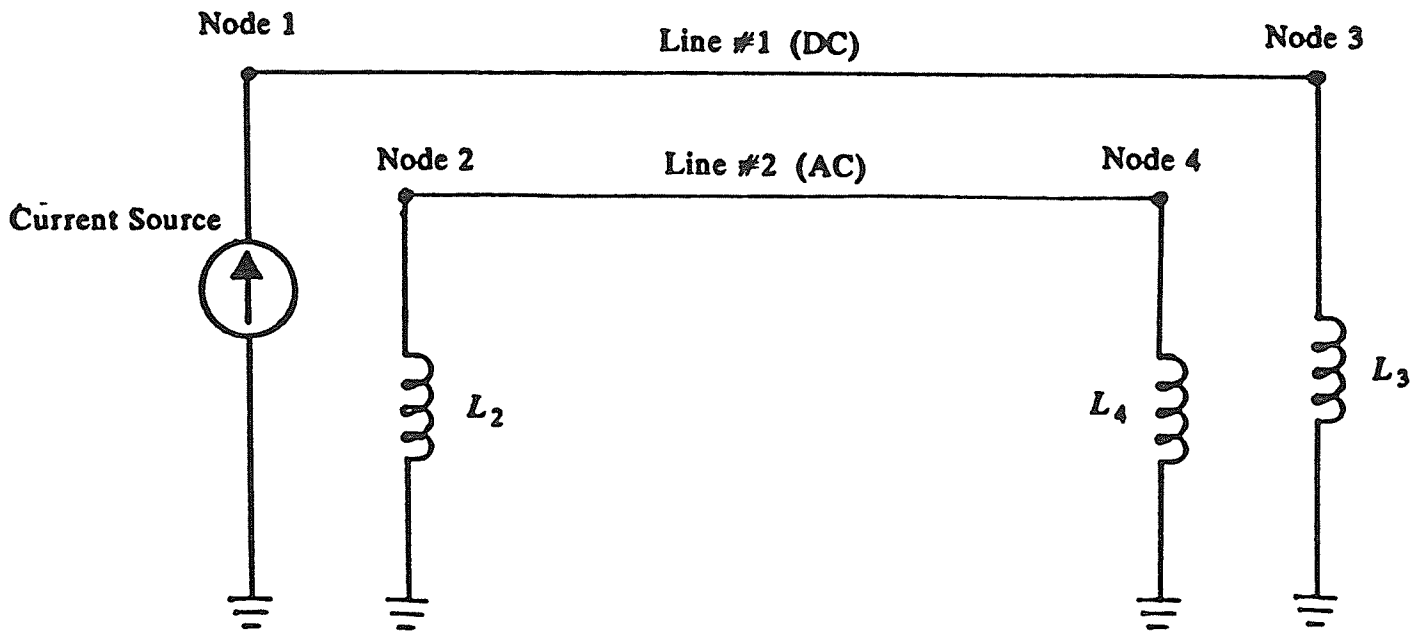


Fig. 3.2 A two-port representation of system of fig. 2.1.

Using (3.11), (3.46) and (3.47), we have

$$\lambda = \begin{bmatrix} 0.9530 \times 10^{-3} + j 0.1660 \times 10^{-13} & 0 \\ 0 & -0.5788 \times 10^{-13} + j 0.5453 \times 10^{-14} \end{bmatrix} \quad (3.50)$$

Also, from equation (3.12), we can write

$$E_v = \begin{bmatrix} 0.9229 - j 0.6197 \times 10^{-1} & 1.0000 - j 0.3725 \times 10^{-8} \\ 1.0000 + j 0.0000 & -0.8160 + j 0.5508 \times 10^{-1} \end{bmatrix} \quad (3.51)$$

Now from equation (3.19), we have

$$\Gamma = E_v \sqrt{\lambda} E_v^{-1} \quad (3.52)$$

Use of (3.50) and (3.51) in (3.52) gives

$$\Gamma = \begin{bmatrix} 0.2026 \times 10^{-7} + j 0.2700 \times 10^{-6} & 0.8496 \times 10^{-8} + j 0.3635 \times 10^{-7} \\ 0.7523 \times 10^{-8} + j 0.3214 \times 10^{-7} & 0.1785 \times 10^{-7} + j 0.2807 \times 10^{-6} \end{bmatrix} \quad (3.53)$$

Inversion of Z-matrix from (3.43) produces

$$Z^{-1} = \begin{bmatrix} 1063.00 - j 7867.00 & 63.51 + j 2056.00 \\ 63.51 + j 2056.00 & 927.00 - j 8277.00 \end{bmatrix} \quad (3.54)$$

From equation (3.24), Y_0 can be calculated as follows

$$Y_0 = Z^{-1} \Gamma =$$

$$\begin{bmatrix} 0.2080 \times 10^{-2} + j 0.1451 \times 10^{-3} & -0.2809 \times 10^{-3} + j 0.2631 \times 10^{-4} \\ -0.2809 \times 10^{-3} + j 0.2631 \times 10^{-4} & 0.2265 \times 10^{-2} + j 0.1322 \times 10^{-3} \end{bmatrix} \quad (3.55)$$

Now, again from equation (3.19), we have

or

$$E_v^{-1} \Gamma x E_v = \sqrt{\lambda} x$$

or

$$E_v^{-1} \coth(\Gamma x) E_v = \coth(\sqrt{\lambda} x)$$

or

$$\coth(\Gamma x) = E_v \coth(\sqrt{\lambda} x) E_v^{-1}$$

For a system length of $x = l = 800$ km,

$$\coth(\Gamma l) = E_v \coth(\sqrt{\lambda} l) E_v^{-1} \quad (3.56)$$

Use of (3.54) and (3.55) in (3.56) gives

$$\coth(\Gamma L) = \begin{bmatrix} 0.3319 - j 4.604 & 0.0622 + j 0.6292 \\ 0.0552 + j 0.5563 & 0.2680 - j 4.431 \end{bmatrix} \quad (3.57)$$

On similar lines, cosech (Γl) is calculated as follows

$$\text{cosech}(\Gamma l) = \begin{bmatrix} 0.3237 - j 4.713 & 0.0587 + j 0.6144 \\ 0.0521 + j 0.5433 & 0.2607 - j 4.544 \end{bmatrix} \quad (3.57)$$

Multiplication of (3.55) & (3.57), and (3.55) & (3.58) respectively gives

$Y_0 \coth (\Gamma l) =$

$$\begin{bmatrix} 0.1328 \times 10^{-2} - j 0.9685 \times 10^{-2} & 0.7942 \times 10^{-4} + j 0.2569 \times 10^{-2} \\ 0.7942 \times 10^{-4} + j 0.2569 \times 10^{-2} & 0.1159 \times 10^{-2} - j 0.1018 \times 10^{-1} \end{bmatrix} \quad (3.58)$$

$Y_0 \operatorname{cosech} (\Gamma l) =$

$$\begin{bmatrix} 0.1328 \times 10^{-2} - j 0.9908 \times 10^{-2} & 0.7935 \times 10^{-4} + j 0.2570 \times 10^{-2} \\ 0.7935 \times 10^{-4} + j 0.2570 \times 10^{-2} & 0.1159 \times 10^{-2} - j 0.1043 \times 10^{-1} \end{bmatrix} \quad (3.59)$$

Using (3.41) and due to the size of matrices, the two-port equations for our system is written as

$$\begin{bmatrix} I_1 \\ I_2 \\ I_3 \\ I_4 \end{bmatrix} = \begin{bmatrix} y_{11} & y_{12} & -y_{13} & -y_{14} \\ y_{21} & y_{22} & -y_{23} & -y_{24} \\ -y_{31} & -y_{32} & y_{33} & y_{34} \\ -y_{41} & -y_{42} & y_{43} & y_{44} \end{bmatrix} \begin{bmatrix} V_1 \\ V_2 \\ V_3 \\ V_4 \end{bmatrix} \quad (3.60)$$

where

$$\begin{bmatrix} y_{11} & y_{12} \\ y_{21} & y_{22} \end{bmatrix} = \begin{bmatrix} y_{33} & y_{34} \\ y_{43} & y_{44} \end{bmatrix} = Y_0 \coth (\Gamma l) ; \text{ given in equation (3.58)}$$

$$-\begin{bmatrix} y_{13} & y_{14} \\ y_{23} & y_{24} \end{bmatrix} = -\begin{bmatrix} y_{31} & y_{32} \\ y_{41} & y_{42} \end{bmatrix} = Y_0 \operatorname{cosech} (\Gamma l) ; \text{ given in equation (3.59)}$$

The end conditions in our case are as follows

$$I_1 = 1 \text{ ampere} \quad (3.61)$$

$$V_2 = I_2 (j \omega L_2) \text{ volts} \quad (3.62)$$

$$V_3 = I_3 (R_3 + j\omega L_3) \text{ volts} \quad (3.63)$$

$$V_4 = I_4 (j\omega L_4) \text{ volts} \quad (3.64)$$

L_2, L_3, L_4, R_3 are known from Table (2-1). Using equations (3.58) to (3.64), the equation (3.60) is solved for I_2, I_3, I_4 to give

$$I_2 = -0.2403 + j 0.04316 \text{ or } 0.2441 \text{ amperes}$$

$$I_3 = -1.037 + j 0.003237 \text{ or } 1.0370 \text{ amperes}$$

$$I_4 = 0.2403 - j 0.04315 \text{ or } 0.2441 \text{ amperes}$$

Thus it is found that with the data given in Table (2-1), 0.2441 ampere (24%) is induced in the line 2 due to 1 ampere current in the line 1 at a frequency of 10 hz and with a ground resistivity of 100 ohm-metre. The qualitative reasoning is provided in Chapter 4.

The whole set of calculations can be repeated at some other frequency or with some other changed parameters. But it is rather impossible if we want to see the response of the system say from 1 hz to 10^6 hz. For this a computer program is required. In the next chapter, a digital simulation program is developed to analyze our model under different conditions.

CHAPTER 4

PARAMETRIC STUDY

ON

A SIMPLIFIED MULTICONDUCTOR SYSTEM MODEL

WITH GROUND RETURN

4.1 Introduction

In the last two chapters, the theory of analyzing a multiconductor system was presented and with its help, a simple multiconductor system shown in Fig. (2.1) of chapter 2 was solved for the data given in table (2-1) of the same chapter. The system was studied for only one frequency. To study the system behavior at different frequencies and with the other parameters changing, a computer program is required. A digital simulation program is developed for simulating the same system as shown again here in Fig. (4.1). Though a two conductor system was chosen for simplicity, the model can handle any number of conductors. The model was tested for its validity and found to be working properly. A number of simulation runs were carried out with different parameters changing and interesting results were recorded and are presented in this section. Later on a slightly different version of the model was developed to take into account the ground wires associated with multiconductor system. A standard fast fourier transform is also incorporated to analyze the time domain input signals.

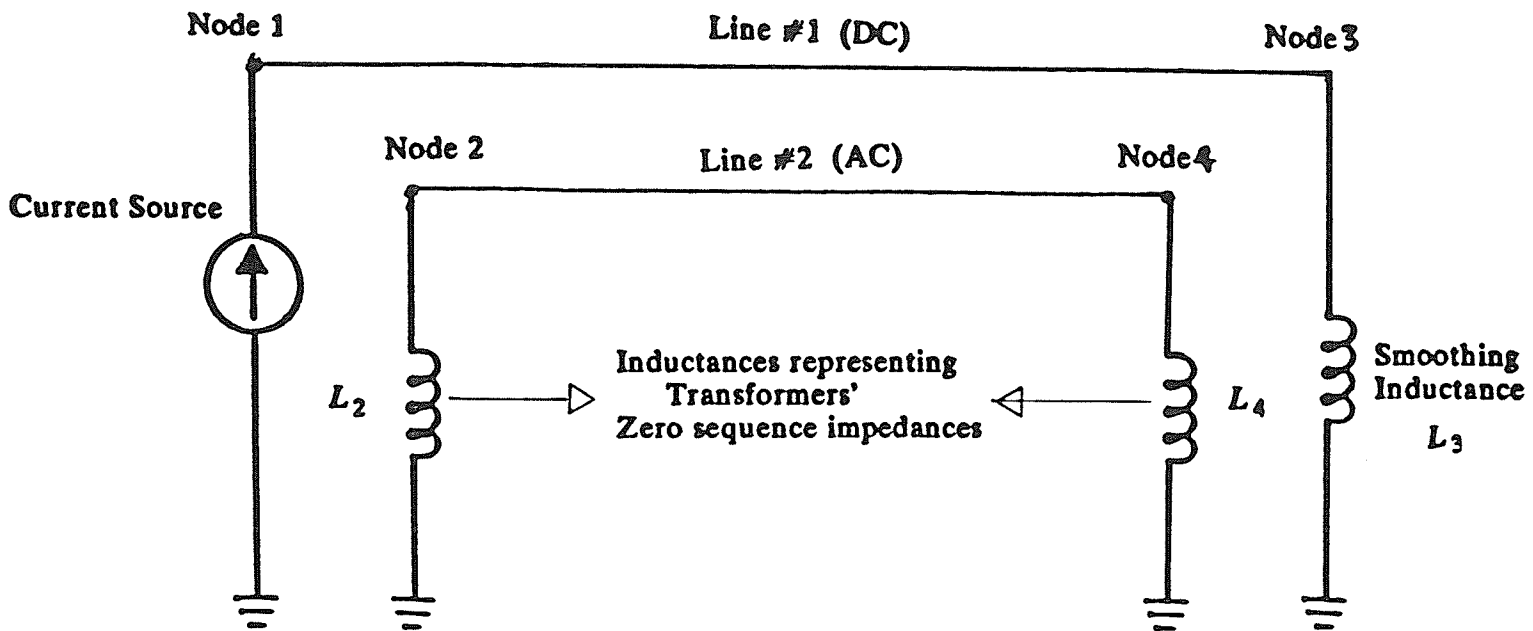


Fig. 4.1 A simplified two-conductor system with ground return.

4.2 Digital Simulation of a Multiconductor System with Ground Return

A digital simulation program is developed to study the induction effects in a multiconductor system with ground return. The purpose of developing this model in this report is to study the currents induced in a line due to the transient currents in the nearby lines at low frequencies. The model works in the frequency domain though a fast fourier transform is added to analyze the time domain input signals. There are two versions of the model, one analyzes the system with ground wire while the other does not handle the ground wire. The theory used in the model has already been explained in chapters 2 and 3. A particular case of a simplified system as shown in Fig. (4.1) was also shown there. The input/output data for the model without ground wire is as follows

- (i) number of conductors. (input)
- (ii) physical geometry of the conductors i.e. the distance between the conductors, height above the ground etc. (input)
- (iii) actual radius of each conductor. (input)
- (iv) geometric mean radius in case of a bundled conductor. (input)
- (v) resistivity of each conductor. (input)
- (vi) ground resistivity. (input)
- (vii) contact resistance between the conductor and the ground. (input)
- (viii) end conditions of the lines depending upon which are required to be known and which are already known. End conditions involve

- (a) currents and voltages at the sending and receiving ends
(input/output)
- (b) line terminating impedance. (input)
- (ix) (a) frequency range of interest. (input) or
- (b) time domain input signal. (input)

In the version which includes the ground wires, the number of ground wires in a system is to be fed as input in addition to the above mentioned input/output data.

To observe the induction effects in a multiconductor system at lower frequencies and with the change of other parameters involved such as ground resistivity etc., tests were conducted on the system of Fig. (4.1) so far we are using in this report. The input required for the system is provided in table 4-1. But before we proceed with a parametric study, it is necessary to test the simulation program for its proper working. In the next section a simple test and its results are described to check the validity of the program.

Table 4-1 Input data describing the system shown in fig (4.1)				
S. no	Description	Quantity	Units	Remarks
1	Number of Conductors	2	nos	
2	Type of Conductor 1	-	-	Aluminum bundled conductor having 2 conductors in it
3	Type of Conductor 2	-	-	-do-
4	Actual radius of each conductor in the bundle (a) Conductor 1 (r_1) (b) Conductor 2 (r_2) (c) Ground conductor	0.02032 0.0254 0.0127	metres metres metres	
5	Geometric mean radius of (a) Conductor 1 (GMR_1) (b) Conductor 2 (GMR_2)	0.0681554 0.1077631	metres metres	
6	Resistivity of (a) Conductor 1 (h_1) (b) Conductor 2 (h_2) (c) Ground conductor	$.28248 \times 10^{-7}$ $.28248 \times 10^{-7}$ $.0471 \times 10^{-7}$	ohm-metre ohm-metre ohm-metre	
7	Spacing between conductors 1 and 2 (S)	182.88	metres	
8	Height above ground of (a) Conductor 1 (h_1) (b) Conductor 2 (h_2) (c) Ground conductor	18.288 14.0208 15.0208	metres metres metres	
9	Ground Resistivity (ρ)	-	ohm-metre	As desired
10	Frequency (f)	-	hz	As desired
11	Current injected at sending end of line 1 (I_1)	-	ampere	This could be of any waveshape form (periodic or non periodic)
12	Terminating inductances (a) L_2 (Transformer) (b) L_3 (Smoothing) (c) L_4 (Transformer)	0.0702 0.5 0.0702	henry henry henry	Inductances are not of much importance at low frequencies
13	The permeability of free space (μ_0)	$4\pi \times 10^{-7}$	henry per metre	
14	The permittivity of free space (k_0)	8.85×10^{-12}	farads per metre	

4.3 Testing of Digital Simulation Program

A short circuit test was performed to check the working of computer simulation program. Under this test, the system of fig. (4.1) shall be modified to that of fig. (4.2). Both the lines are short circuited to ground at their respective ends. A current of 1 ampere was injected at the sending end of line 1 while the other was kept opened at the same end. The test was carried out with a low frequency of 10 hz so that capacitance effect of the line could be ignored. The ground resistivity is assumed to be 100 ohm-metre. Under these conditions voltages at node 1 and at node 2 are given by

$$\begin{bmatrix} V_1 \\ V_2 \end{bmatrix} = - \begin{bmatrix} z_{11} & z_{12} \\ z_{21} & z_{22} \end{bmatrix} \begin{bmatrix} I_1 \\ I_2 \end{bmatrix}$$

Since

$$I_1 = 1 \text{ ampere}$$

$$I_2 = 0$$

$$|V_1| = |Z_{11}|, \text{ the self impedance of line 1}$$

$$|V_2| = |Z_{21}|, \text{ the mutual impedance between line 1 and 2}$$

The test was performed with the same data of table (2.1) of chapter 2 and the impedance matrix came out as

$$\begin{bmatrix} 0.2069 \times 10^{-4} + j 0.1325 \times 10^{-3} & 0.9703 \times 10^{-5} + j 0.3167 \times 10^{-4} \\ 0.9703 \times 10^{-5} + j 0.3167 \times 10^{-4} & 0.1685 \times 10^{-4} + j 0.1267 \times 10^{-3} \end{bmatrix}$$

i.e.

$$Z_{11} = 0.2069 \times 10^{-4} + j 0.1325 \times 10^{-3} \quad \text{ohms / metre}$$

$$Z_{12} = 0.9703 \times 10^{-5} + j 0.3167 \times 10^{-4} \quad \text{ohms / metre}$$

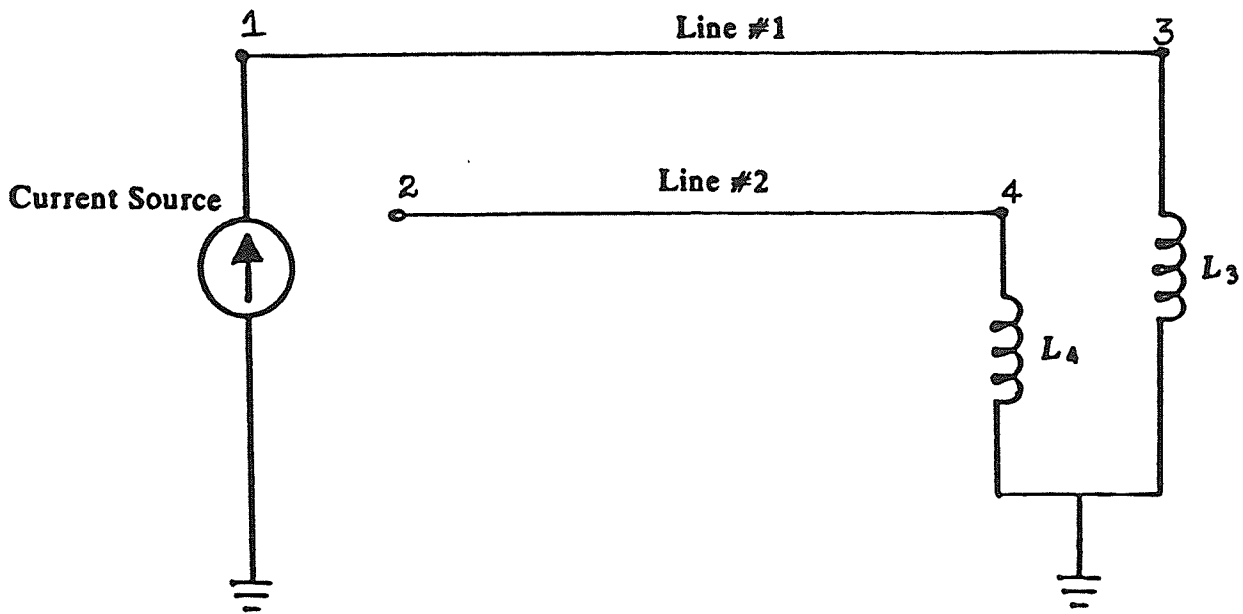


Fig. 4.2 Representation of the system of Fig. 4.1 during short circuit test.

For transmission line of 10 km each,

$$Z_{11} = 0.2069 + j1.325 \text{ ohms and}$$

$$Z_{12} = 0.0970 + j.3167 \text{ ohms}$$

The voltages v_1 and v_2 which are being calculated at the end of entire program came out as expected.

$$V_1 = 0.207 + j 1.325 \text{ volts } (= |Z_{11}|)$$

$$V_2 = 0.0970 + j .3167 \text{ volts } (= |Z_{12}|)$$

The test was repeated with other frequencies and ground resistivities and the results were found to be satisfactory. To an extent this confirmed the correctness of the computer program.

4.4 Parametric Studies of the Model

After verifying the computer simulation program, other tests were carried out keeping in view the main problem of induced zero sequence currents in the ac lines due to transients in the nearby dc lines with ground return. The system of fig. (4.1) was simulated under various conditions. The tests and their results are explained below.

4.4.1 Base Case

First of all a base case was run with the data provided in table (4-1). In this case, earth is assumed to be a perfect conductor i.e. ground resistivity is equal to zero. Contact resistances between the ground and the conductors are neglected. The currents were measured and recorded at all the four nodes of the system of fig. (4-1) as shown in fig. (4-3). It can be seen that almost no current is induced at low frequencies. A physical reason for this is given in the following section. The peaks at higher frequencies indicate the effects of inductance and capacitance of the lines and the resonant conditions which are of little interest in the case at hand.

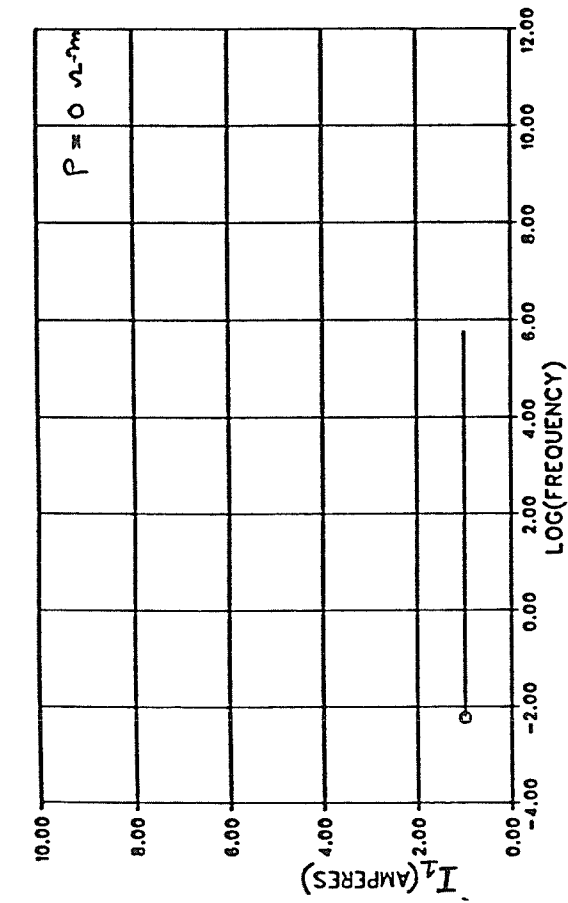


Fig. 4.3 (a)

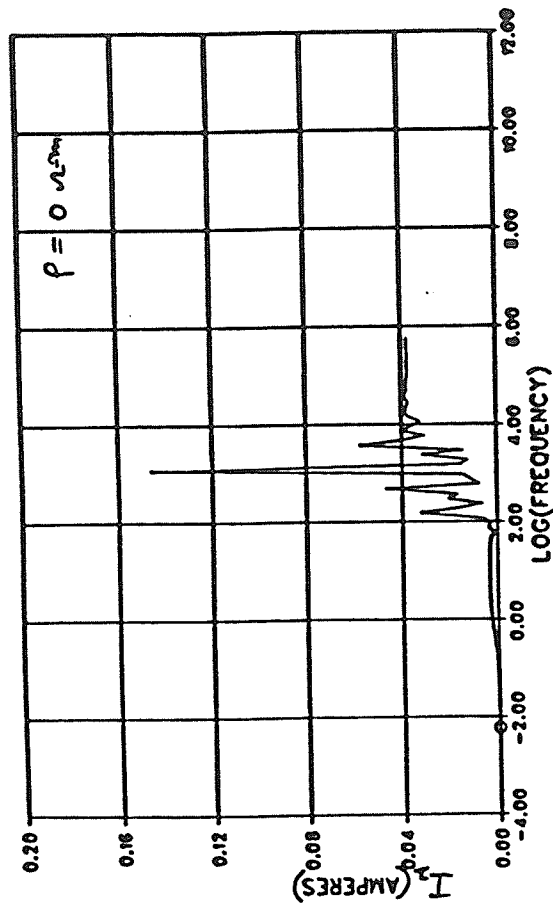


Fig. 4.3 (b)

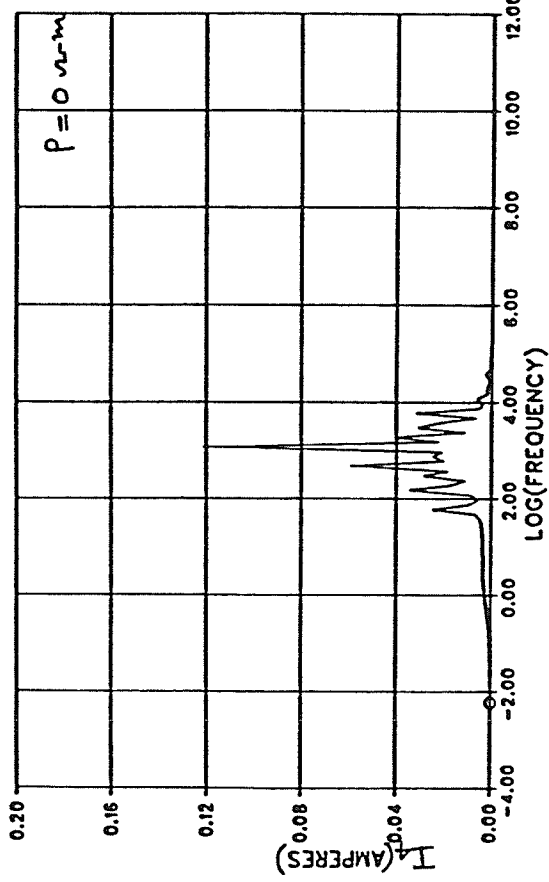


Fig. 4.3 (c)

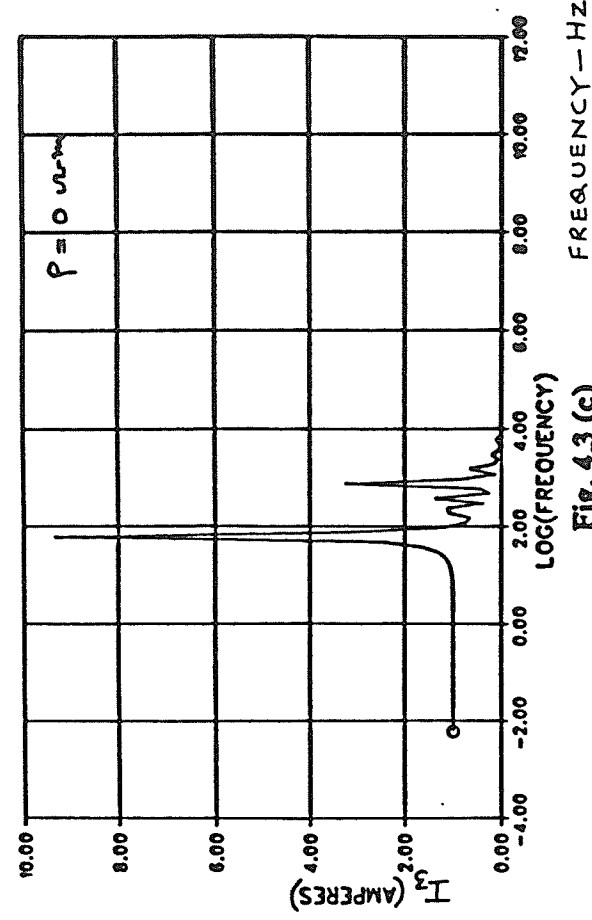


Fig. 4.3 (d)

Fig. 4.3 Frequency response of the system assuming earth to be a perfect conductor.

4.4.2 Effect of Ground Resistivity

A number of simulation runs were carried out considering the practical case of ground being an imperfect conductor. Though the earth is very non-uniform (the surface layers of the land have many local irregularities of differing resistivity, such as rivers, deserts, marshes etc.) yet for simplicity the assumption of uniform earth gives a good starting point for analyzing the problem. With the same data except the ground resistivity used in the base case, the system of Fig. (4-1) was simulated with varying ground resistivity. The system response as recorded in Fig. (4.4) shows that approximately 27% current is induced in line 2 due to current in line 1 at low frequencies. This proves that there exists a fairly strong coupling between the lines at low frequencies even when the lines are sufficiently apart (in the present case they are 200 metres apart). This is attributed due to the reason explained below.

In a transmission system using ground as a return path, the depth of penetration of the current into the ground depends upon its frequency and the ground resistivity and is given by the equation (2.17) of chapter (2).

At zero frequency (direct current) or at low frequencies the current flows very deep into the ground and spreads over a very large cross sectional area in both depth and width. This return current may be represented as that in an 'image conductor', the location of which is at a depth equal to the depth of penetration below the ground. The two lines with ground as their return paths, and running parallel, may be quite apart, still there is a strong coupling between the two at low frequencies due to the formation of two electromag-

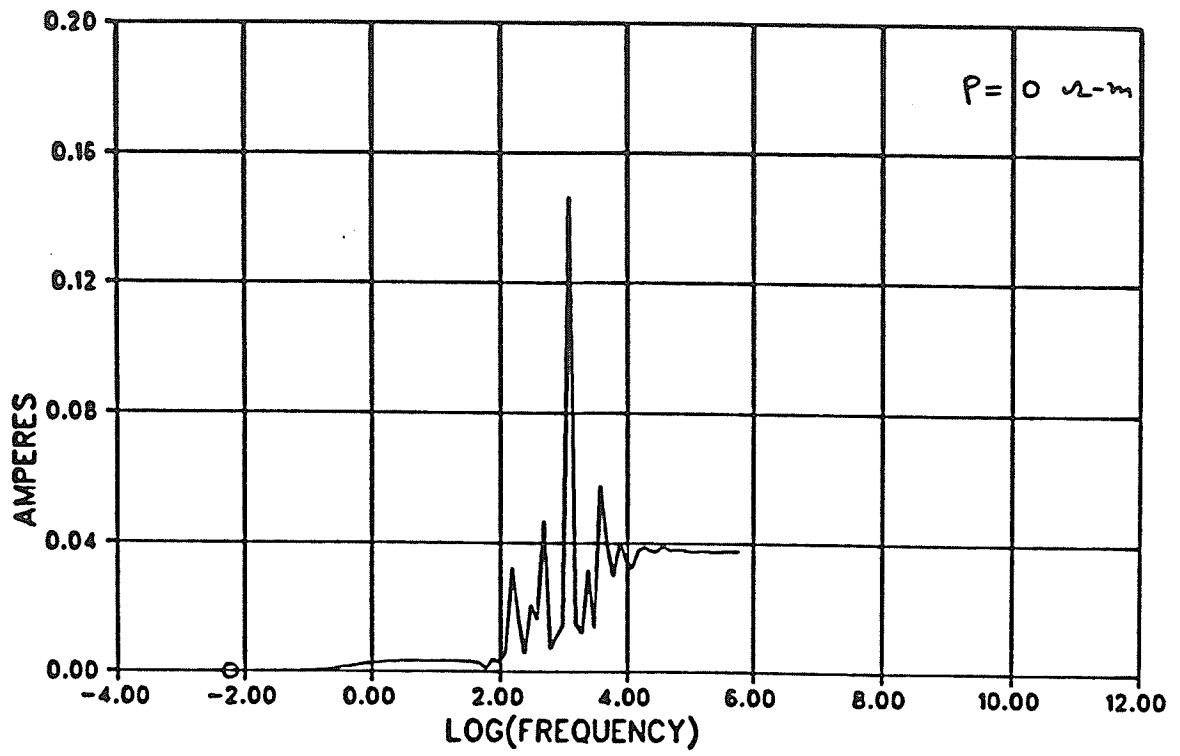


Fig. 4.4 (a)

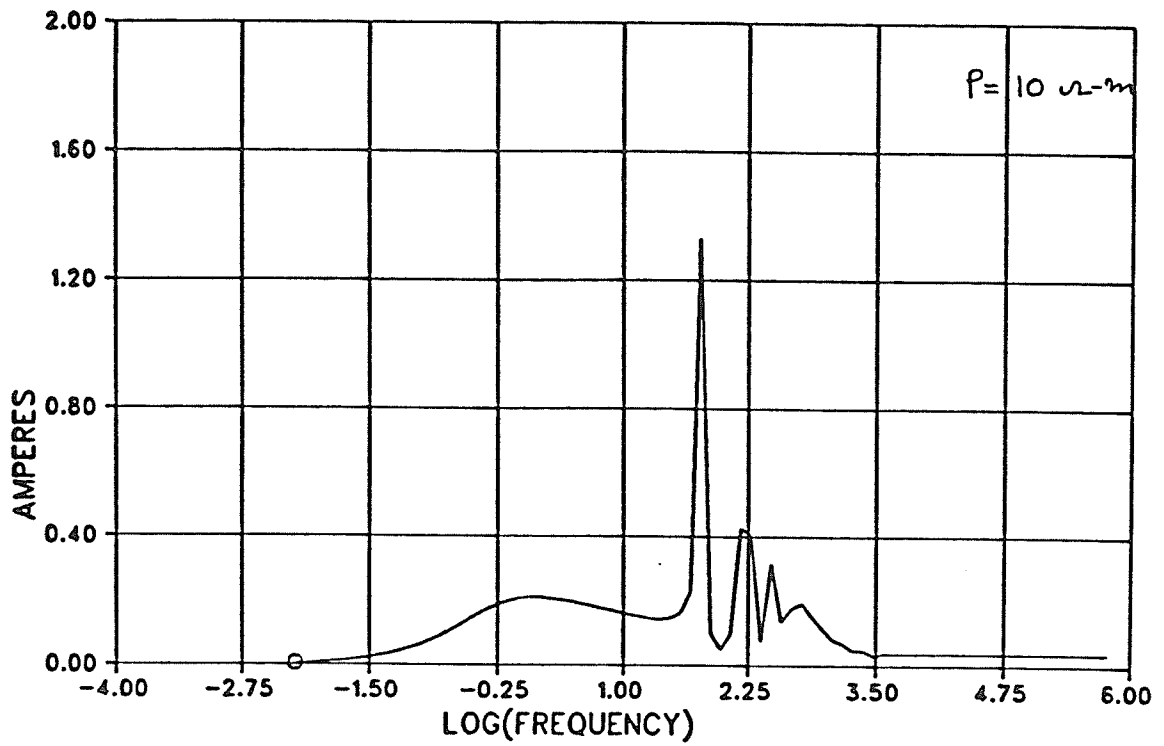


Fig. 4.4 (b)

Fig. 4.4 Frequency response (I_2) of the system considering earth as an imperfect conductor.

....contd.

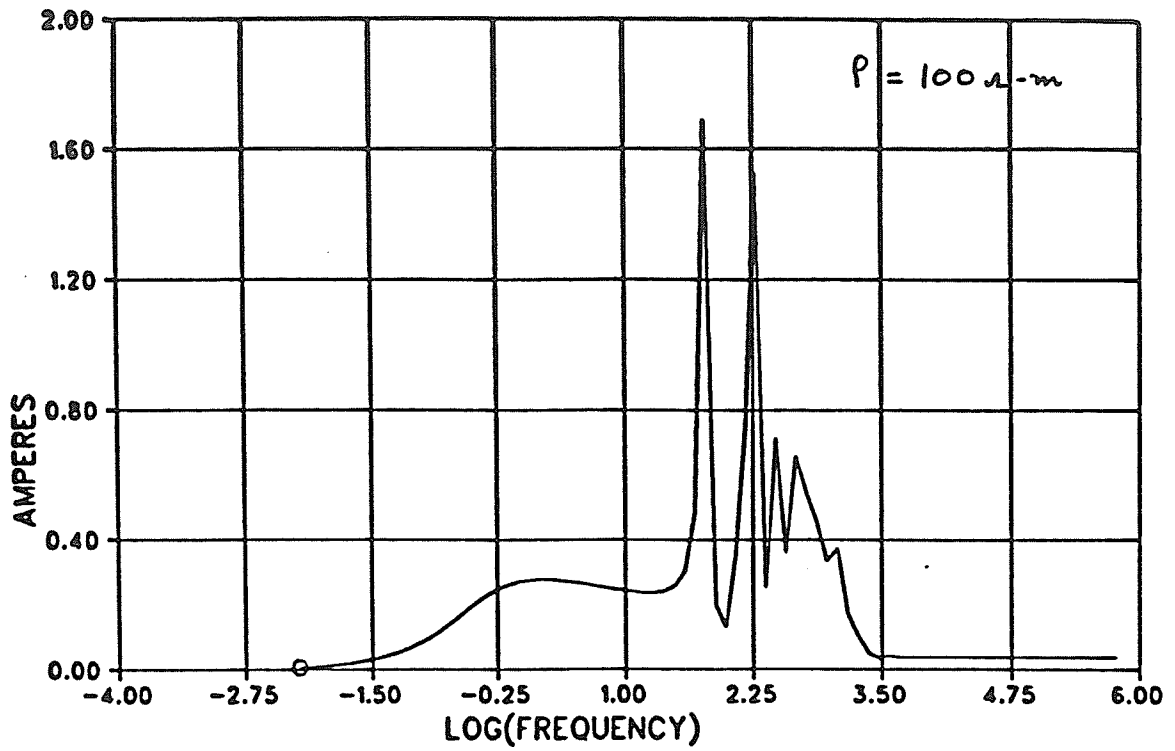


Fig. 4.4 (c)

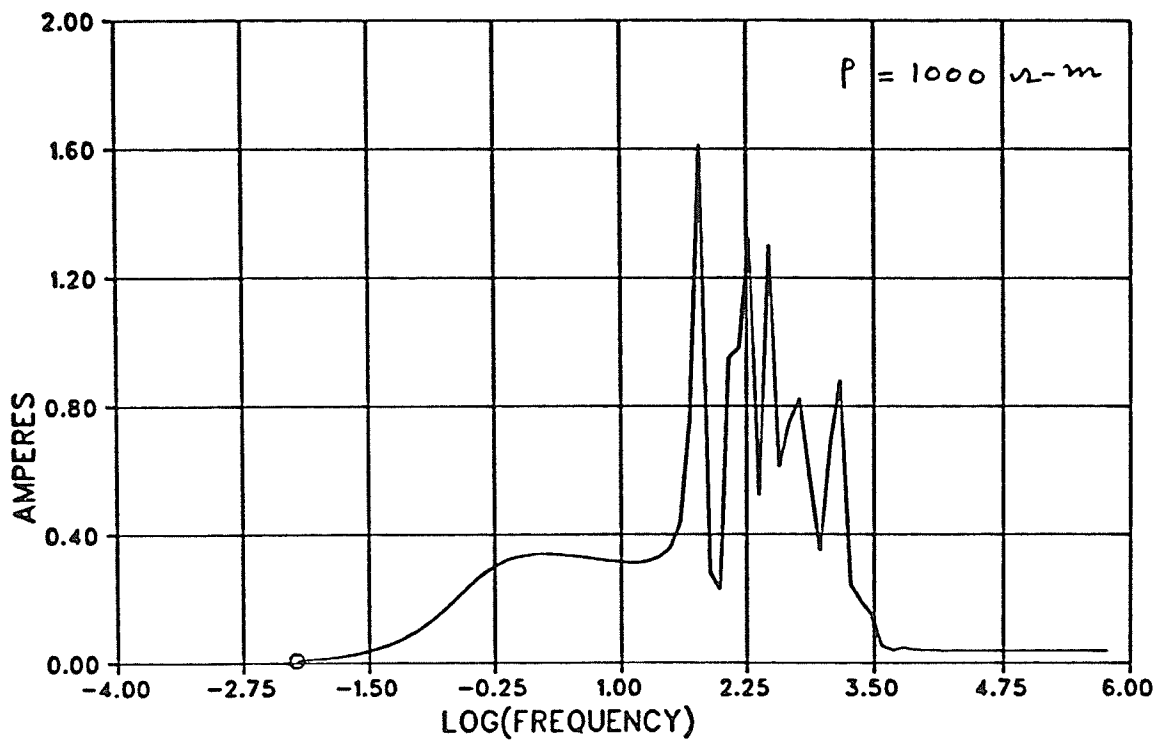


Fig. 4.4 (d)

Fig. 4.4 Frequency response (I_2) of the system considering earth as an imperfect conductor.

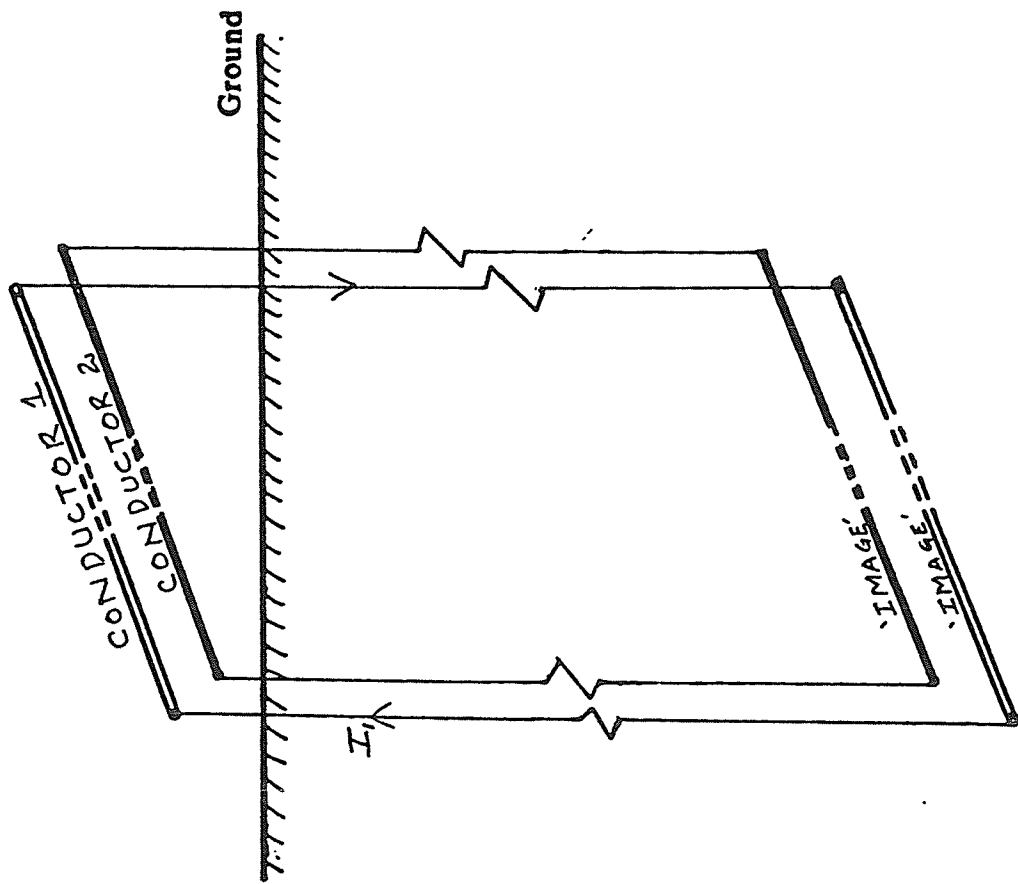


Fig. 4.5(a) Symbolic representation of currents carrying by conductors 1 and 2 (grounded at both ends), flowing deep into the ground at low frequencies.

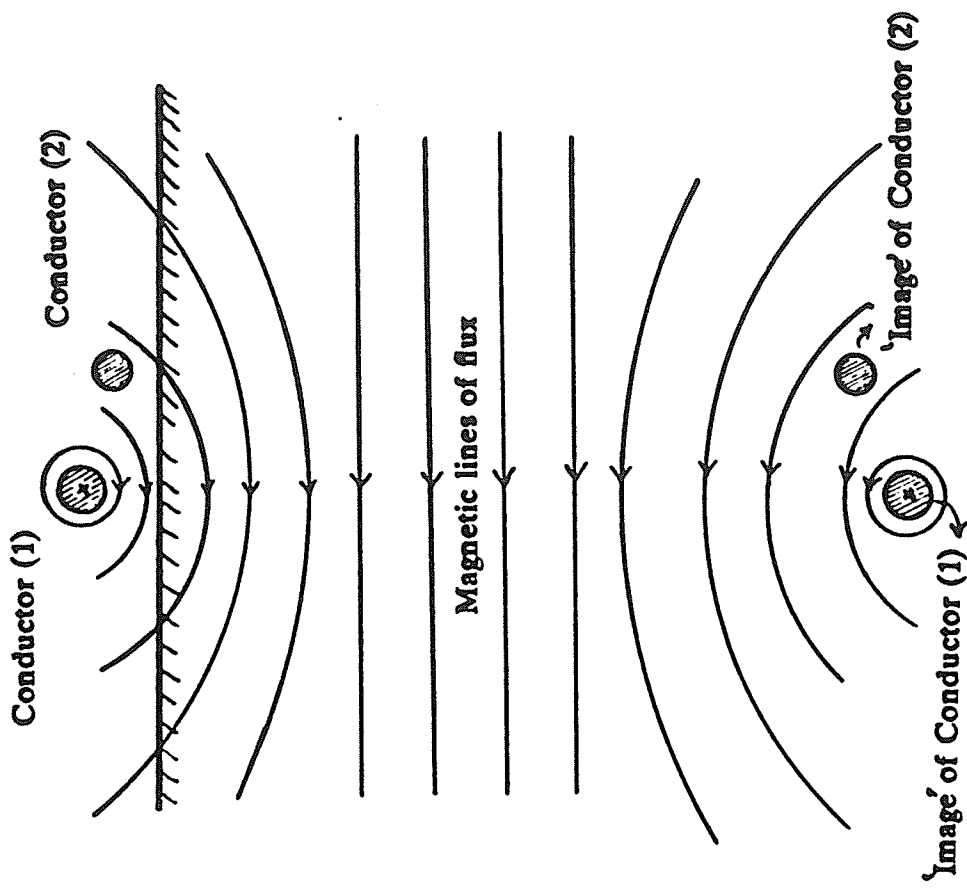


Fig. 4.5(b) Electro-magnetic coupling at low frequencies.

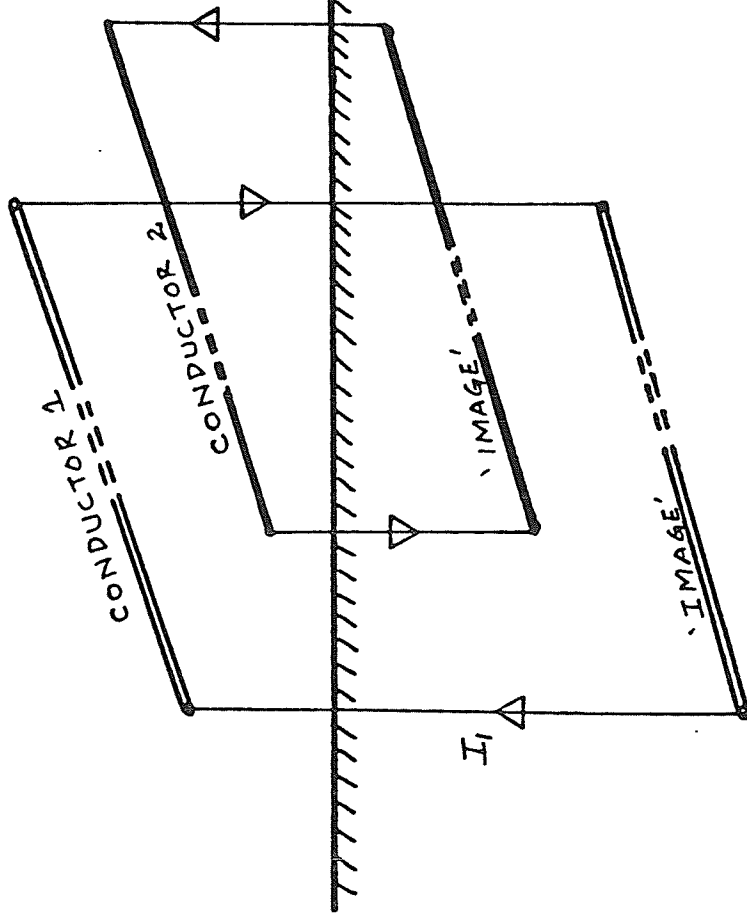


Fig. 4.5(a) Symbolic representation of currents carrying by conductors 1 and 2 (grounded at both ends), flowing nearer to the surface of the ground at high frequencies.

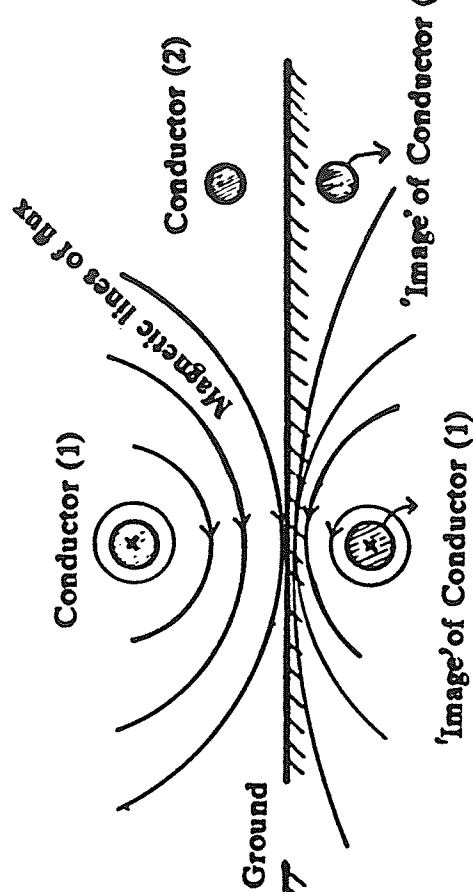


Fig. 4.5(b) Electro-magnetic coupling at high frequencies.

netic coupled loops as shown in Fig. (4.5). The area of the loop is much greater than the separation between the conductors and hence most of the flux linking one loop also links the other, resulting in strong coupling.

Now as the frequency increases (as in the case of transients or alternating current), the current starts flowing nearer to the ground and if the lines are farther apart, the electromagnetically coupled loop shall be formed as shown in Fig. (4.6).

In the case of ground resistivity being exactly zero (superconducting ground), the image depth is exactly equal to the height of the conductor above ground (at any frequency) and so the strong coupling for low frequencies (which appears because of large penetration depths) does not occur in this case. This explains the results of section 4.4.1.

Note also, that the actual induced voltage in the second loop is a function of field coupling as well as rate of change of that field. So at near dc frequencies, though most of the flux links both loops, the rate of change of flux is very small. This voltage, which is the driving force behind the current in the loop therefore drops to zero at low frequencies and consequently so does the current. That is why current induced is quite small at very low frequency (less than 1 Hz) as shown in Fig. (4.4).

4.4.3 Effect of Varying Distance Between the Lines (ac and dc)

The base case was simulated assuming approximately 183 metres distance between the lines. To observe the effects of different distances between the two lines on the induced current, simulation runs were carried out by assuming 50, 183 and 1000 metres as the distance between the two lines respectively. The results are shown in Fig. (4.7). Increase in induction when the lines are just 50 metres apart is not as much of a surprise as the existence of a significant induction at lower frequencies even when the lines are one km apart. This is attributed to the fact that depth of penetration of ground current (which may be several hundred metres) is still quite large as compared to the distance between the lines and consequently resulting in electromagnetically coupled loop as explained in the previous section.

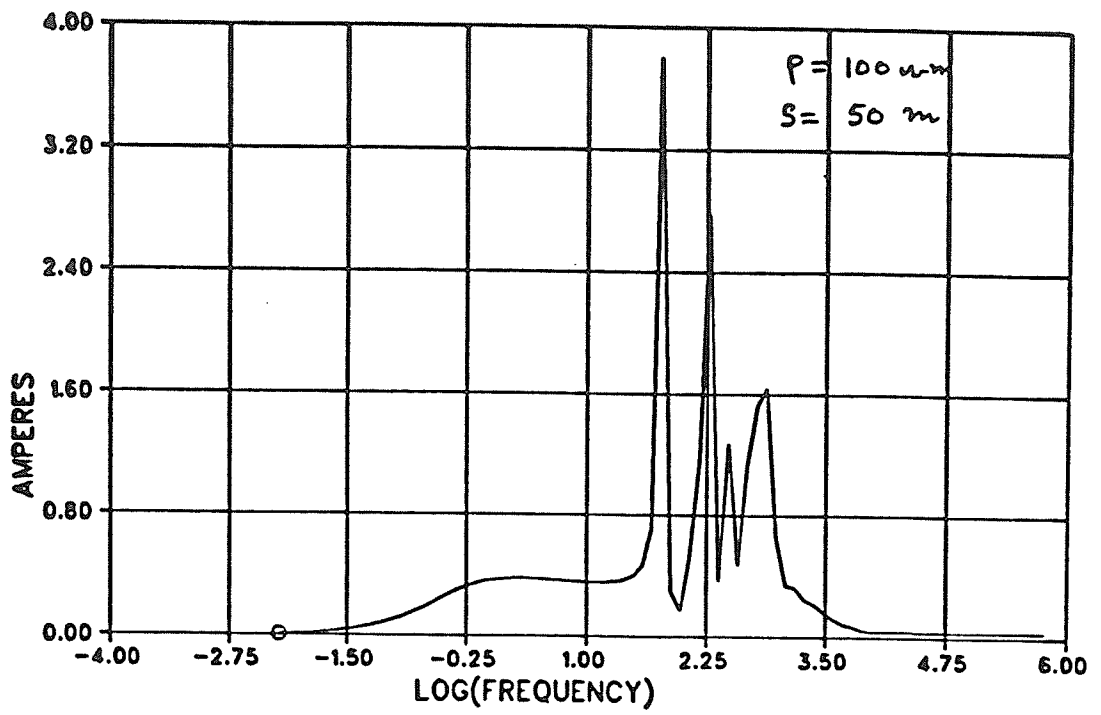


Fig. 4.7 (a)

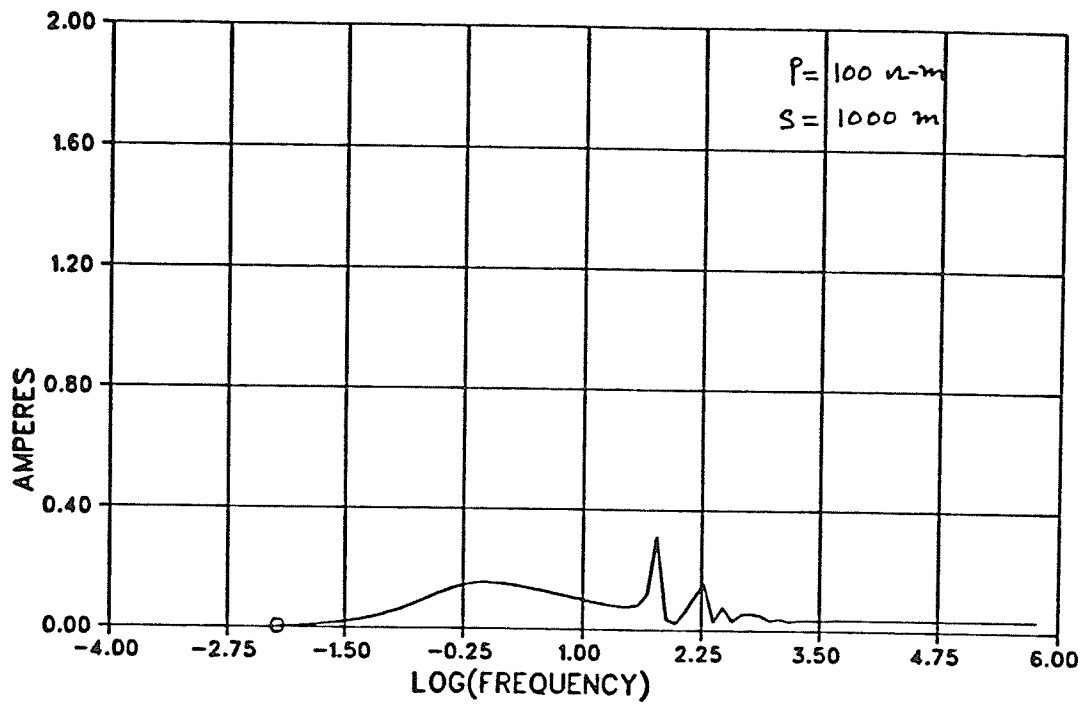


Fig. 4.7 (b)

Fig. 4.7 Variation of induced current (I_2) as the distance between the lines changes.

4.4.4 Effect of Contact Resistance

In a transmission system with ground as a return path, current flow lines are parallel to one another and to the metallic conductors except near the ends of it as shown in Fig. (4.8). At the ends, these current flow lines diverge from, or converge to, the electrode in case of dc transmission or to the station earthing mat in case of ac transmission. This phenomenon is usually known as an 'end effect'.^[11] This effect is predominant in a zone having dimensions of twice or thrice the depth of penetration of the ground current. Both direct and alternating currents follow ground paths which offer the least impedance. For dc, the impedance consists only of resistive component whereas for ac, it has both resistive and reactive components. At low frequencies, only the resistive component will be active. The end effects are taken into account by considering resistance in series with the lines at their ends as shown in Fig. (4.9). As mentioned earlier for dc (at zero frequency), the ground currents spread deep below the ground, in which case nothing is left but the end effects. In that case the resistance of the ground return is merely the sum of the resistances associated with each electrode. In ac transmission with ground return, the earthing mat at the generating stations has typical resistance (contact resistance) of .5 to 4 ohms. However, it depends upon the ground resistivity at which the station is located.

Simulation runs were carried out with different values of contact resistances and the results were recorded as shown in Fig. (4.10). Fig. (4.10 b) shows that as contact resistance increases, there is higher damping effect,

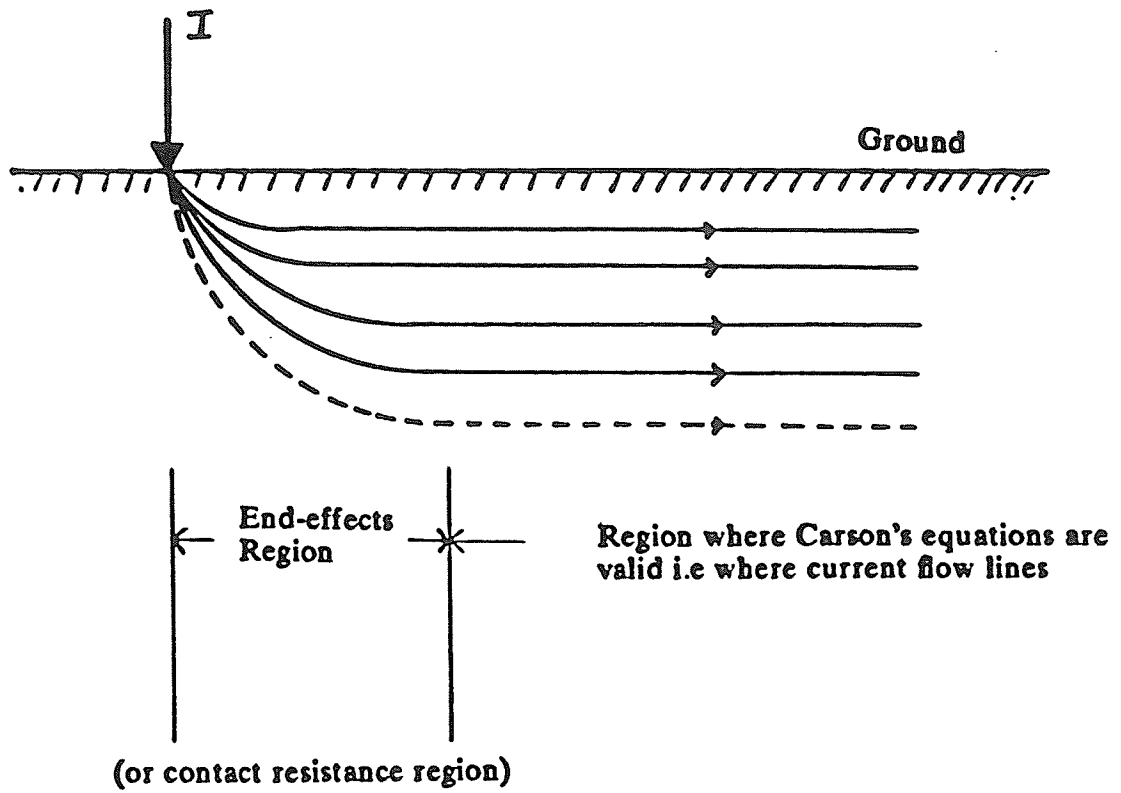


Fig. 4.8 End-effects phenomenon.

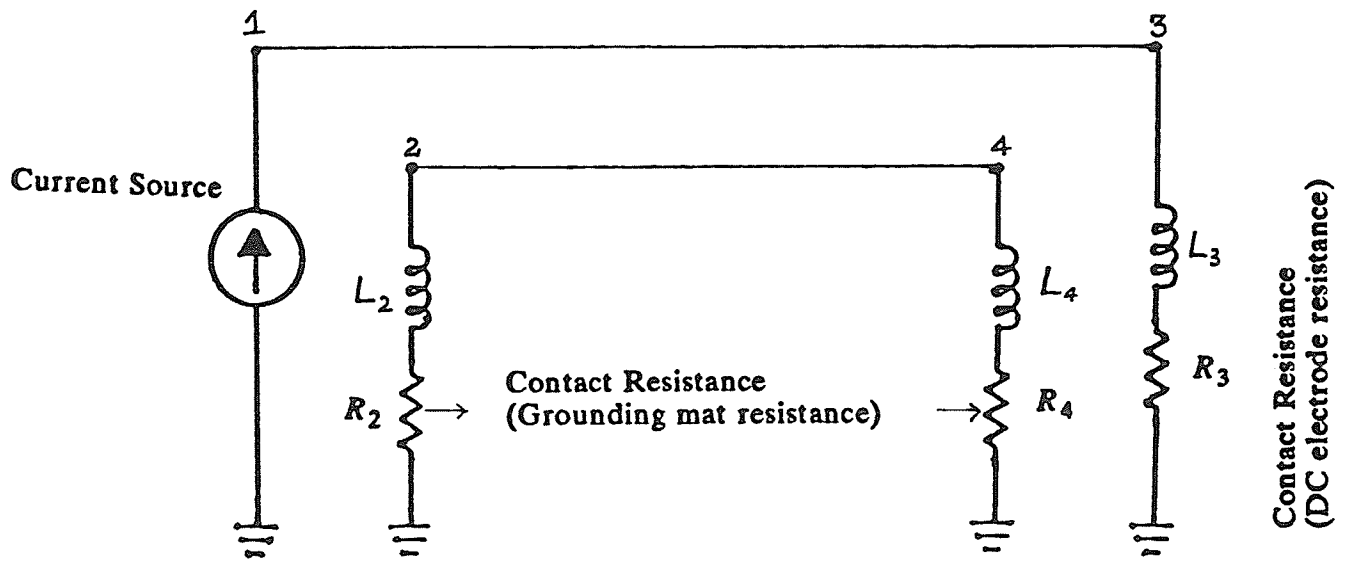


Fig. 4.9 Representation of model taking contact resistance into account.

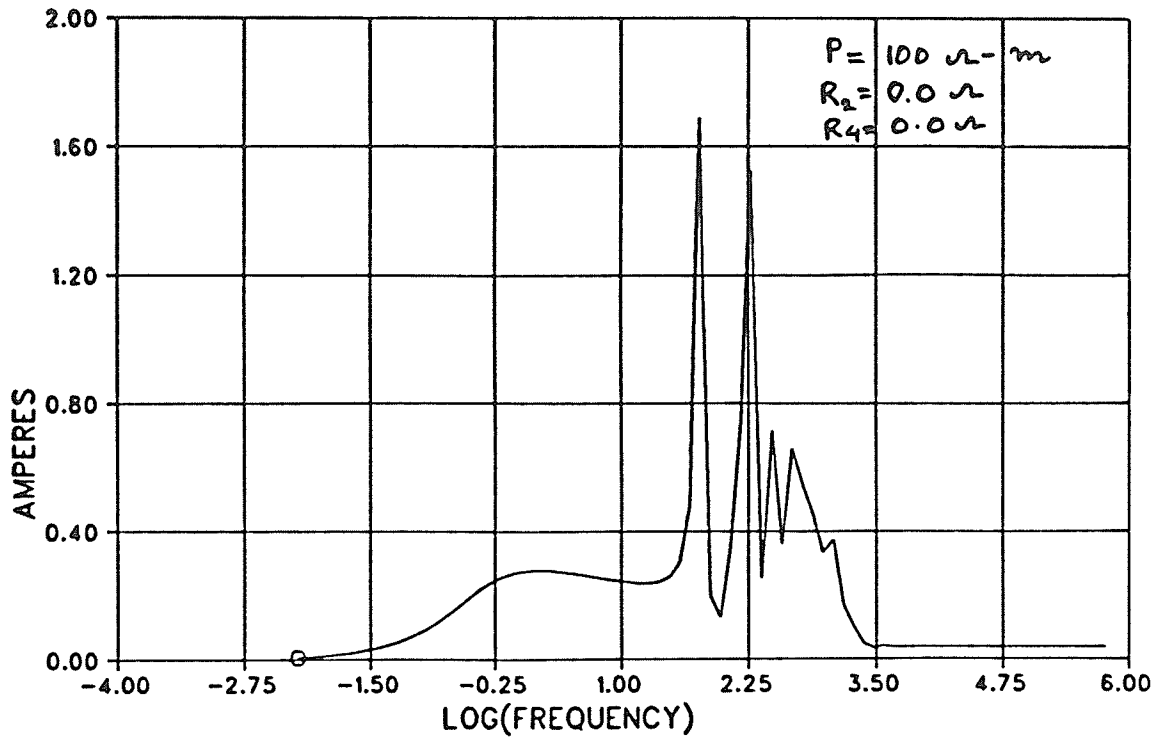


Fig. 4.10(a)

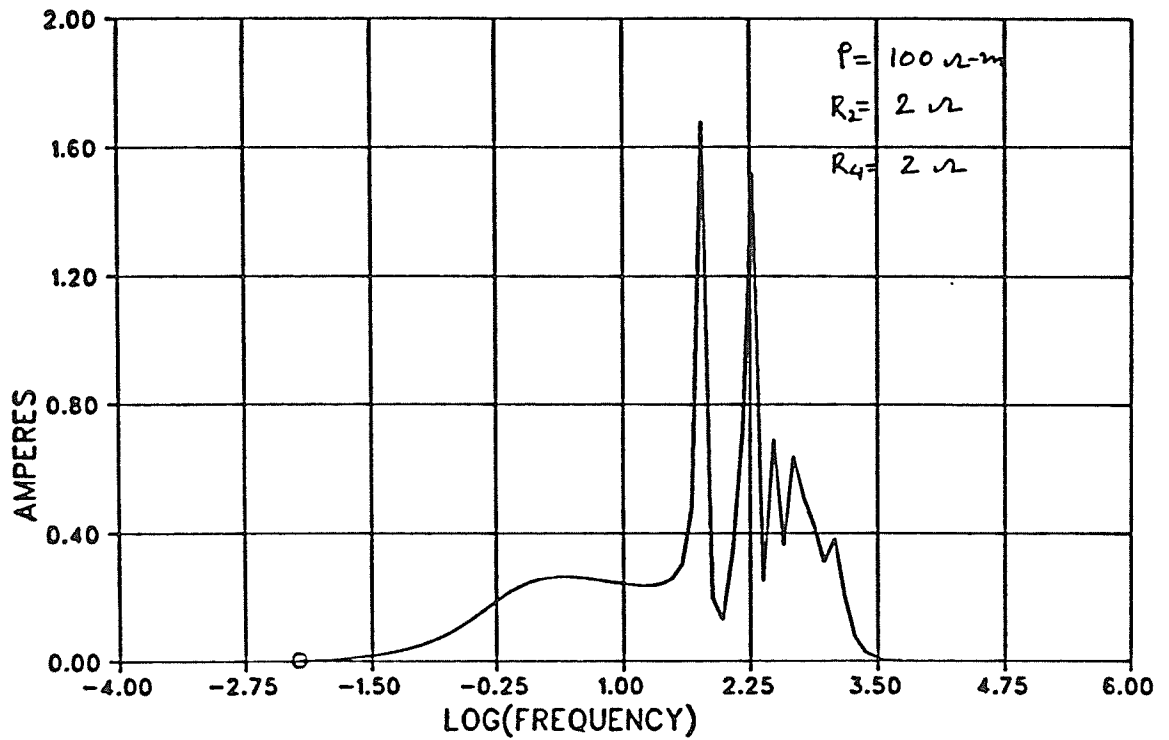


Fig. 4.10(b)

Fig. 4.10 Effect of contact resistance on induced current (I_2).

resulting in lower time constant of decay for the induced current. This fact can be observed more explicitly in time domain analysis carried out in a further section.

4.4.5 Effect of Mutual Contact Resistance

Initially a theory based upon the mutual contact resistance was thought to be the cause for induction effects at lower frequencies. The mutual contact resistance is nothing but considered as to account for common ground path shared by the current I_1 and I_2 shown in Fig. (4.11). The model was simulated with some typical values of R_m and without R_m . The results recorded are shown in Fig. (4.12). It can be seen from Fig. (4.12 b) that at nearly zero frequency, there is a significant amount of current induced in line 2. However, unlike the observed induced current (by Manitoba Hydro), the induced current calculated by this theory has a dc component. Therefore mutual contact resistance does not explain the observed phenomenon, and must be discarded. The theory explained in section 4.4.2, therefore, seems more applicable.

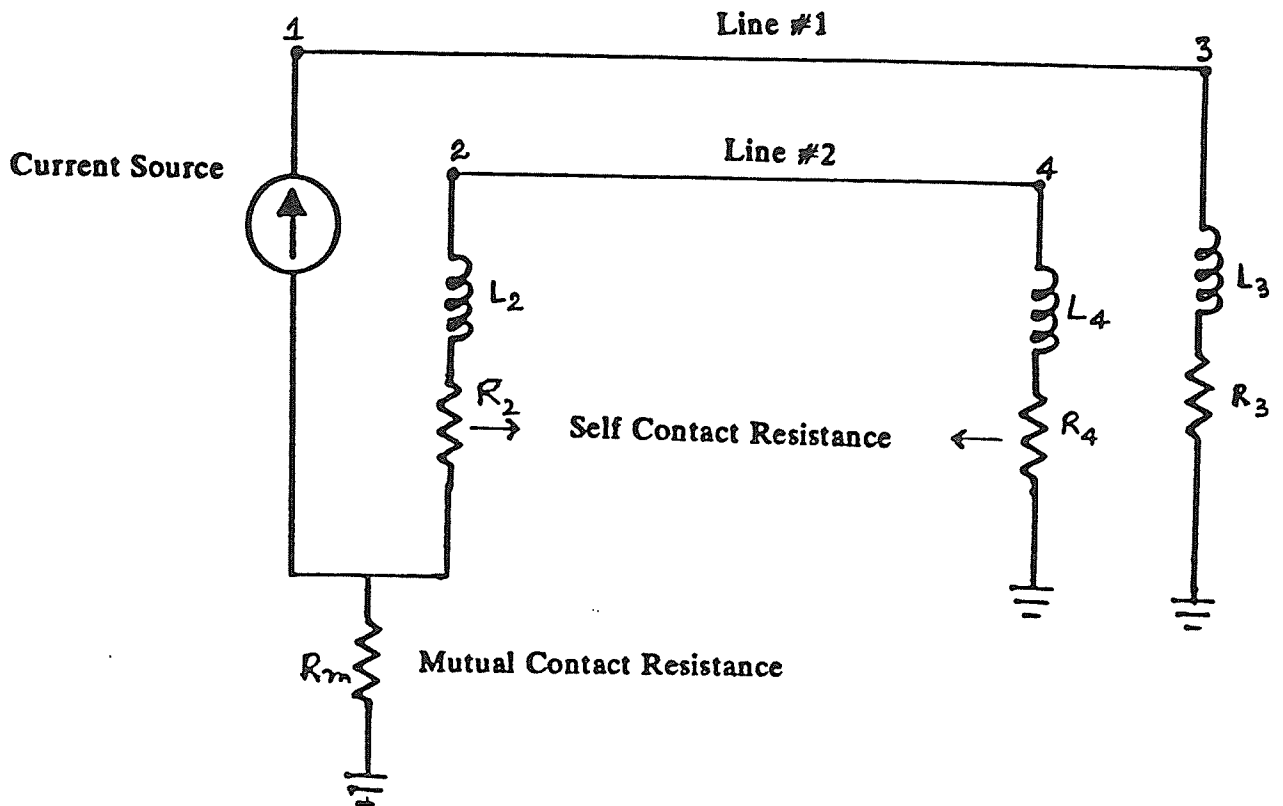


Fig. 4.11 System representation, taking self and mutual contact resistances into account.

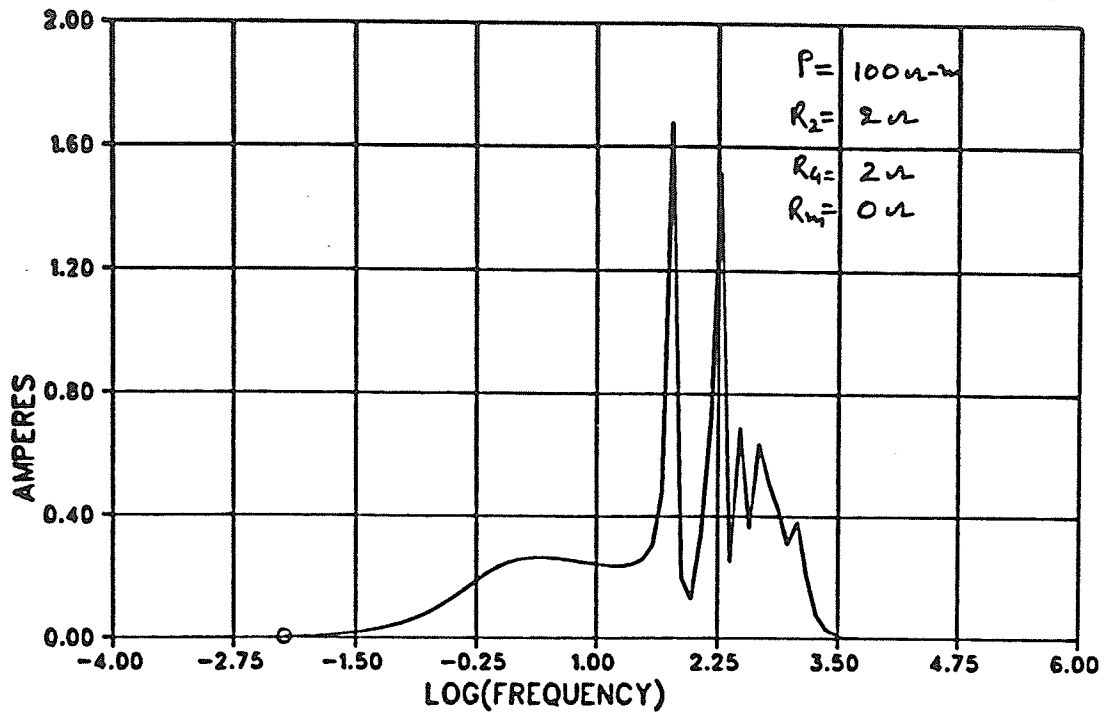


Fig. 4.12(a)

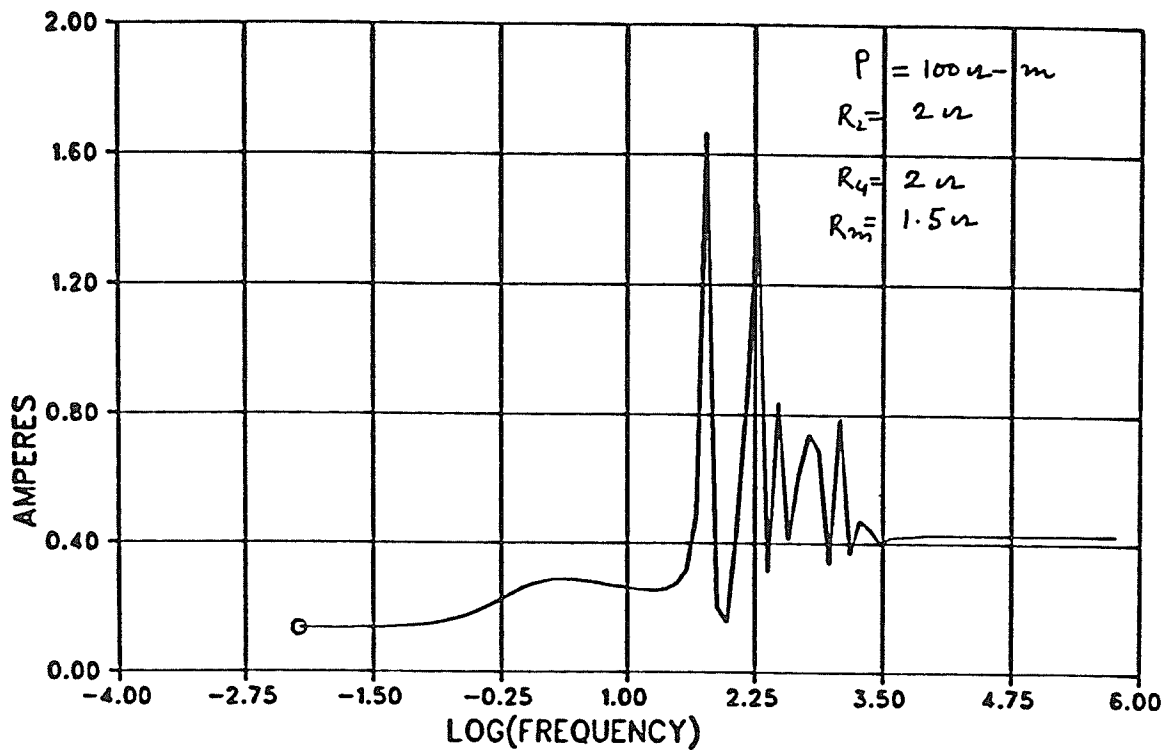


Fig. 4.12 Effect of mutual contact resistance on induced current(I_2).

4.4.6 Effect of Ground Wires

Usually overhead lines are protected from direct strokes of lightning by one or more wires at ground potential strung above the power line conductors. The zone of protection is normally considered to be 30° on each side of vertical beneath a ground wire. To observe the effect of ground wires present in the system on induction between the two lines, a simulation run was carried out with the data of Table (2-1). It is assumed that the line 2 (ac) carries a ground wire above it as shown in fig. (4.13). It was found that ground wires in the system did not have any appreciable effect on the induction between the two lines. The frequency response of the system with and without ground wire is shown in fig. (4.14). About 4% reduction in the induced current (I_2) was observed at ground resistivity of 100 ohm-metre.

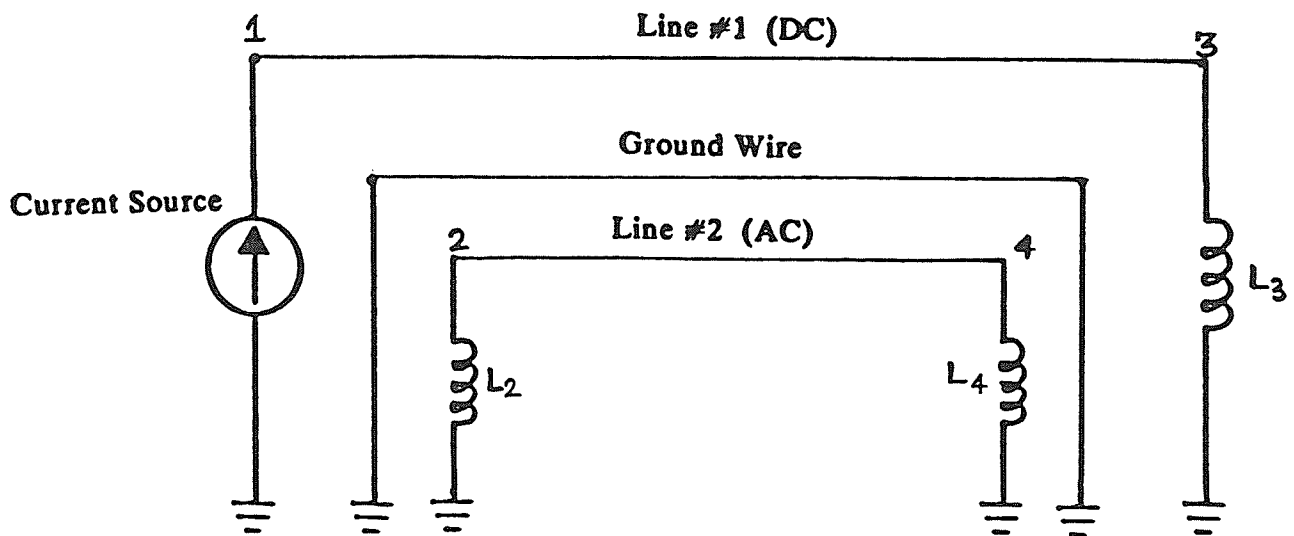


Fig. 4.13 System representation with a ground wire on line # 2

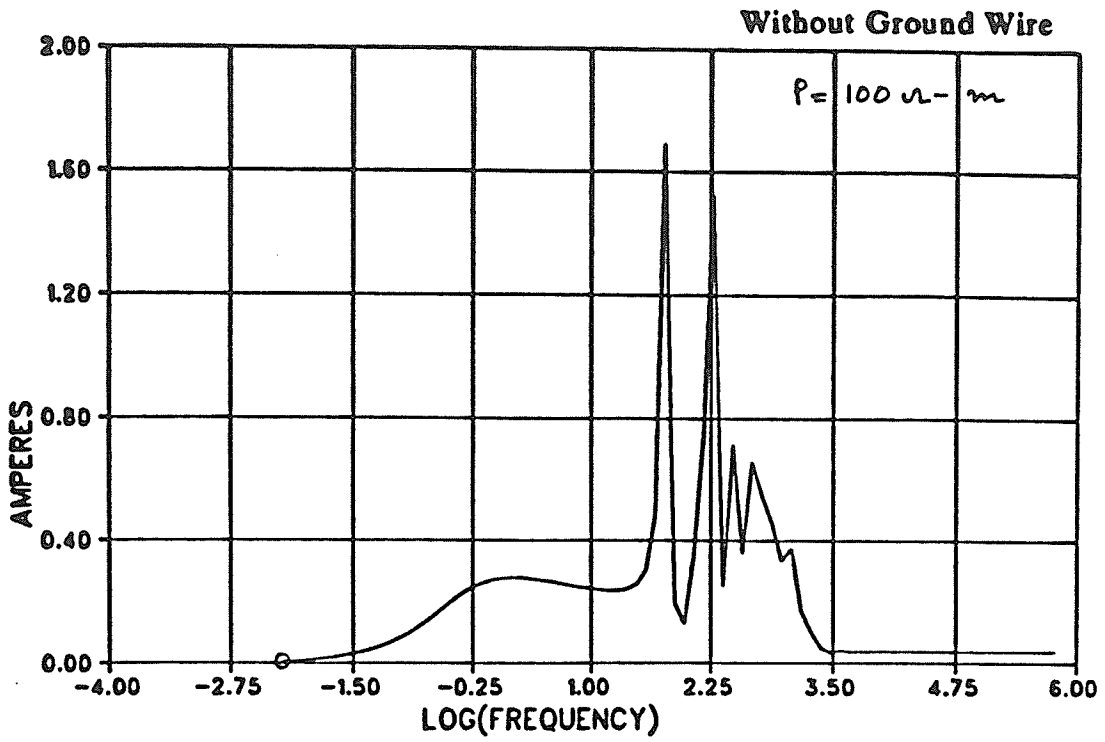


Fig. 4.14(a)

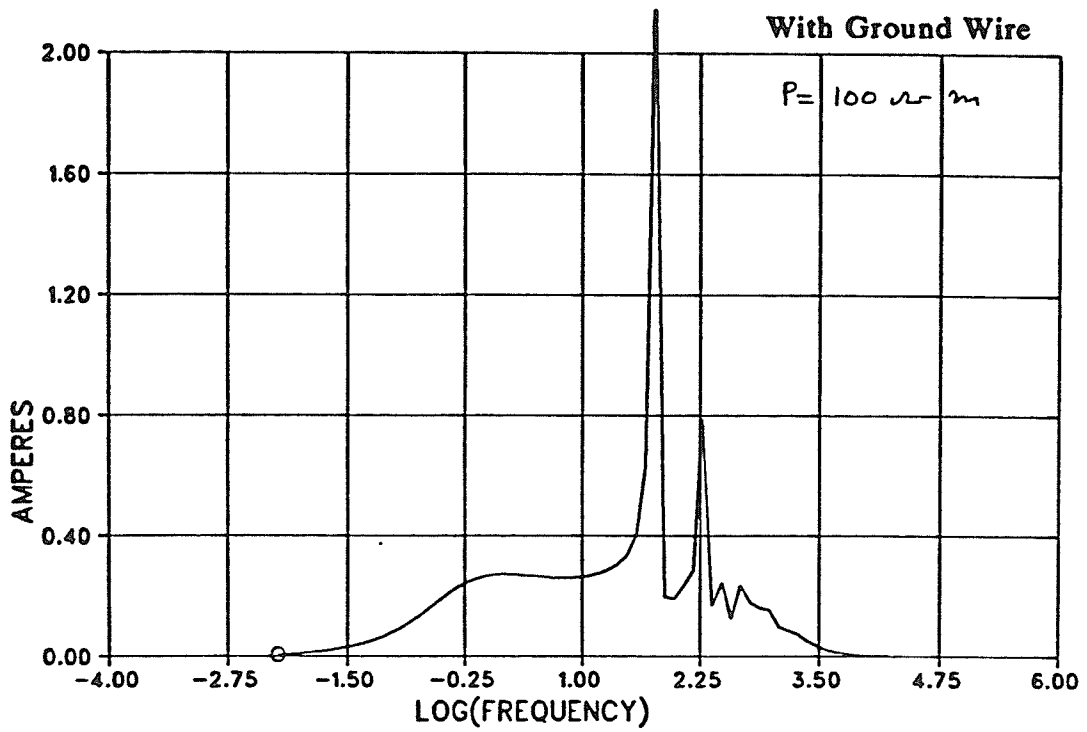


Fig. 4.14(b)

Fig. 4.14 Frequency response (I_2) with ground wire present in the system.

4.5 Response of the System with time-domain input current signal

In the previous sections, the model was analyzed with a sinusoidal current of 1 ampere magnitude, injected into the dc line. The aim was to study the basic phenomenon involved in the main problem. In this section efforts are being made to study the response of the system to an input current signal, similar to the actual one recorded during the parallel operation of the dc valve groups by Manitoba Hydro. The waveshape of the recorded signal is in time domain. To analyze the system (which is in frequency domain) to an input time domain signal, a standard fast fourier transform $FFT^{[12]}$ is included into simulation program as explained below.

So far the digital simulation program was calculating the response of the system to a given input frequency domain signal over a certain range of frequencies. To deal with an input time domain signal $i(t)$, the first task would be to transform this into its frequency components such as $I_1(\omega_1)$, $I_1(\omega_1)$ etc. through a standard FFT program. The procedure is illustrated in block diagram (4.15). Then, as before, the simulation program would calculate $I_2(\omega)$, $I_3(\omega)$, $I_4(\omega)$ corresponding to each frequency component. To get time domain output signal (or response), all the respective frequency components of $I_2(\omega)$, $I_3(\omega)$, $I_4(\omega)$ are fed into a standard inverse FFT program.

The number of points in FFT has been chosen in such a way so as to avoid wrap around error^[12] in the time domain response. For this, an estimate of the time constant (τ) of the system to dc was made from Fig. 4.17 and the number of points (N) were selected so that

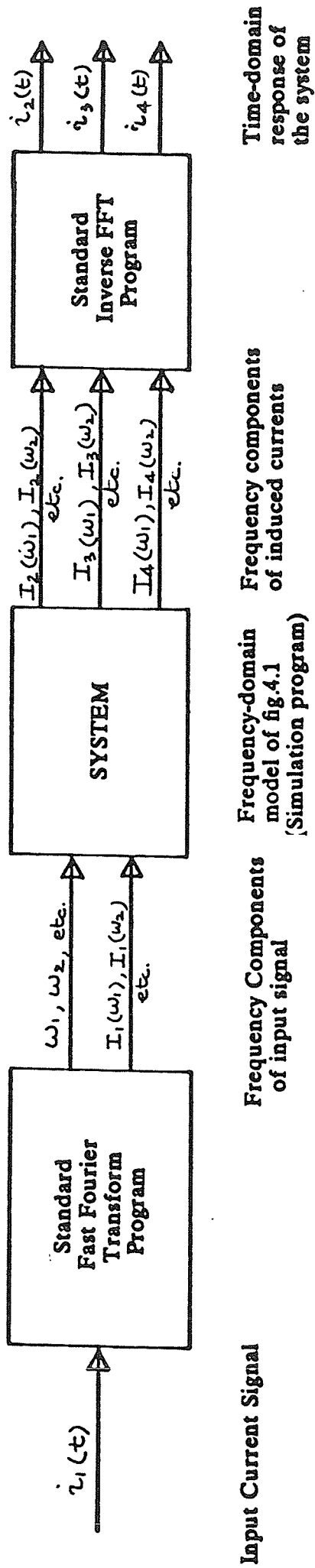


Fig. 4.15 Block diagram showing sequences involved in getting response of the frequency-domain model to a time-domain input current signal.

$$N \times T_s \geq 3\tau$$

where T_s is the sampling time or time between two consecutive points. This would prevent wrap around error (or inverse aliasing). This is just analogous to the necessity of obeying the sampling theorem in frequency domain to avoid aliasing. Further, a rectangular window was used in time domain, but as long as the window width $N \times T_s \gg 3\tau$, it really would not make any difference even if some other window is being used.

The input signal $I_1(\omega)$ in the present case is band limited (to 1 kHz), therefore $I_1(\omega).G(\omega)$, where $G(\omega)$ is the frequency response of the system, shall also be band limited to 1 kHz. As we are actually interested in the inverse transform of $I_1(\omega).G(\omega)$ i.e. time response of the system, we do not require any special window in the frequency domain up to $1/T_s$, which is 2 kHz (> 1 kHz). In other words, the sampling theorem is to be followed to avoid aliasing.

An approximation of the actual recorded current signal by Manitoba Hydro is shown in Fig. (4.16). It can be seen that before current gets stabilized, there is a sharp rate of change of current (from 1800 amperes to 4000 amperes) during a very short interval of time. During this transient period, the nearby ac lines running parallel to the dc lines got tripped. An analysis was carried out with a similar input current signal.

The input current signal shown in Fig. (4.16) was applied to the system under consideration with the data given in table (4-1). The system response is recorded in Fig. (4.17). It is observed that the induced current has the same

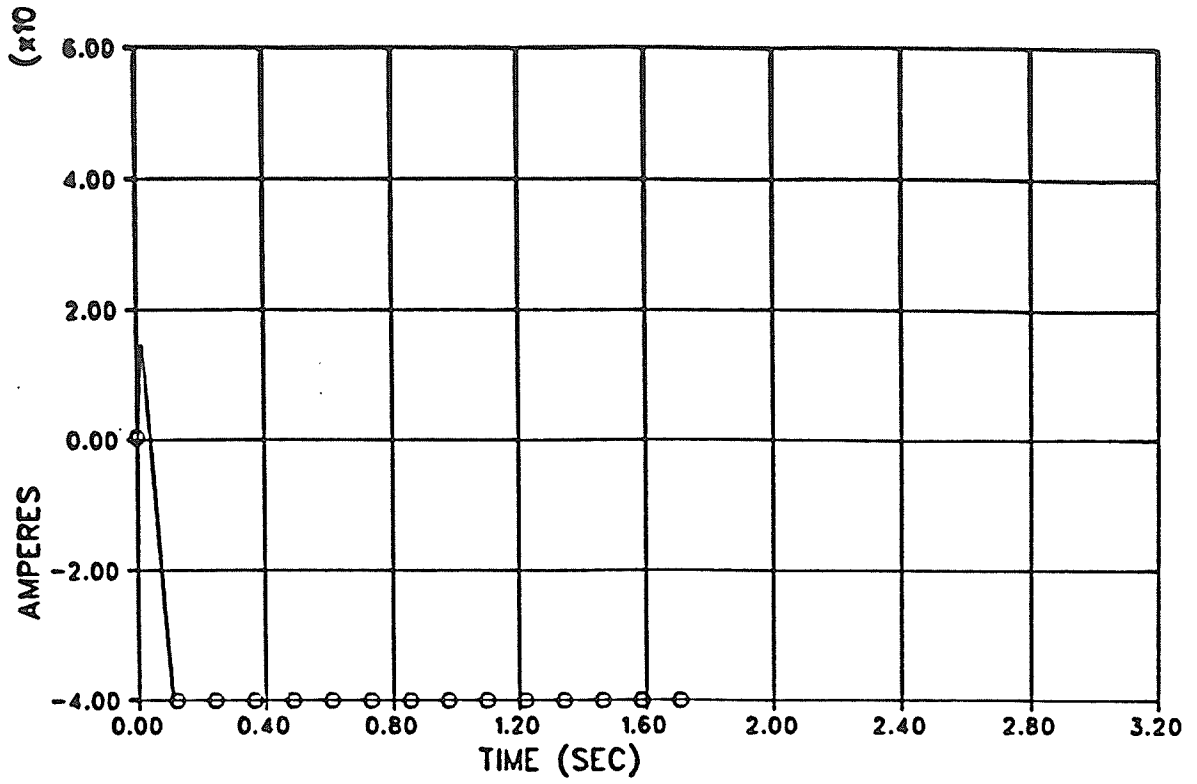


Fig. 4.16 Input Current Signal

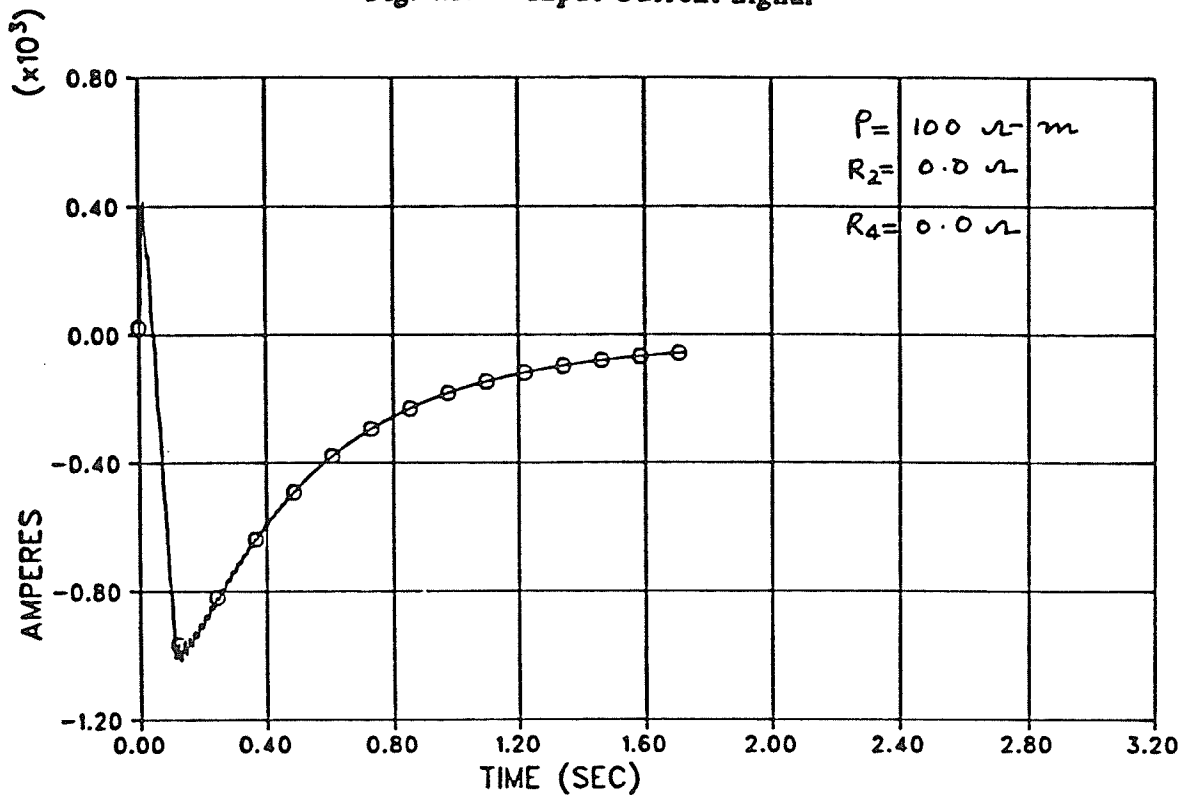


Fig. 4.17 Response of the system (I_2) to the input current signal of Fig. 4.16 .

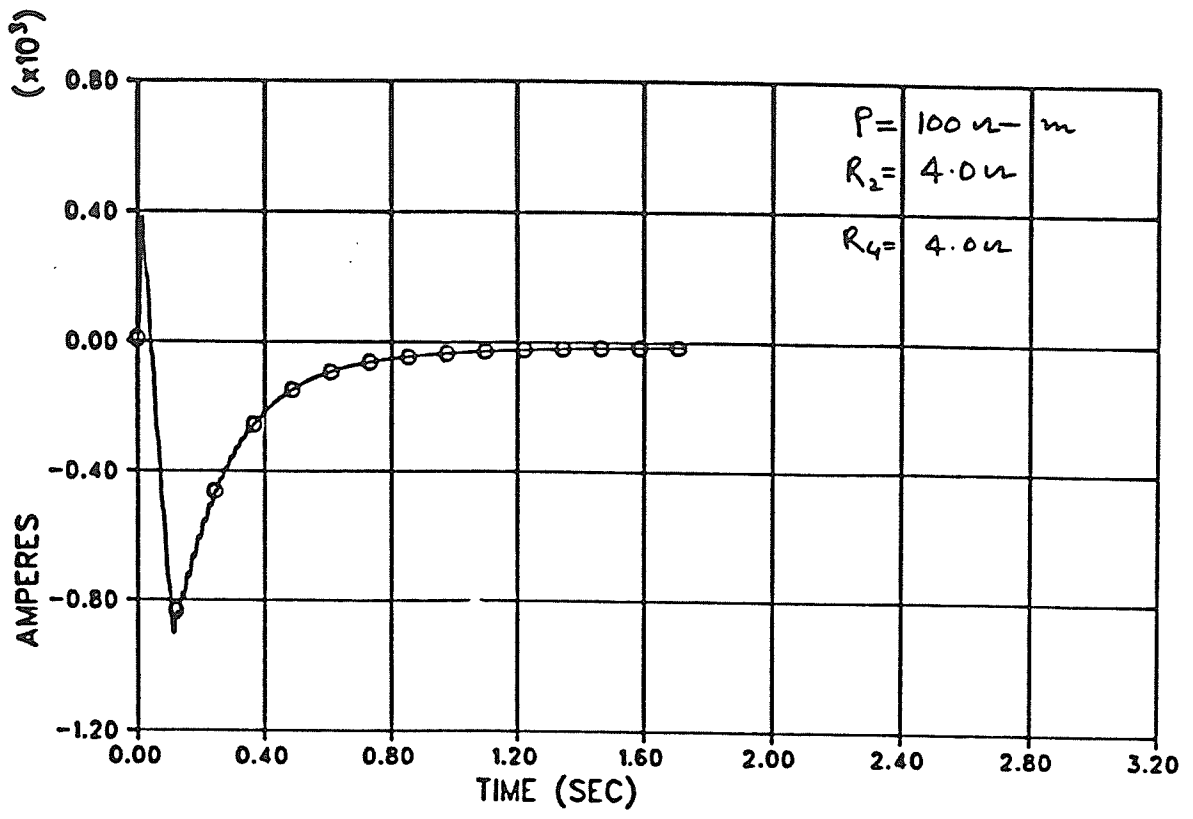


Fig. 4.18 Effect of 'contact resistance to ground' on the response of the system (I_2).

initial waveshape as of the input current signal but with a lesser magnitude (approximately 25% of the input current) and dying down exponentially. In this case, the contact resistance is assumed to be negligible and perhaps could be the reason for taking induced current a long time (more than one second) to die down.

Next, the above case was repeated with some typical values of contact resistances for ac ground mat and dc electrodes and the response obtained is shown in Fig. (4.18). In comparison with the Fig. (4.17) it can be noticed that the decay time of the induced current has been reduced in this case. This is attributed to the lower time constant of decay and higher damping of the circuit due to increased resistance. The overall magnitude of the induced current has also reduced from approximately 25% to 20%. The trend observed here is quite similar to the actual one recorded by Manitoba Hydro. This proves that large currents can be induced in the lines with ground return at low frequency, with decay time as a function of ground resistance.

CHAPTER 5

CONCLUSIONS AND RECOMMENDATIONS

5.1 Conclusions

1. There exists a strong coupling in a multiconductor system using ground as return path at low frequencies even if transmission lines are far apart (say 500 metres or more). As long as the depth of penetration of ground current, which is a function of frequency and ground resistivity, is large as compared to the distance between the lines, the system shall experience a significant coupling in the zero sequence current.
2. The induced current in a line would have much the same initial waveshape as that of the current in another line due to which it occurs, but with less magnitude as shown in figs. 4.17 and 4.18. This is also evident from the frequency response graph of fig. (4.4), which shows constant gain in the low frequency range (.1 - 100 Hz.). At very low frequency (dc), however, the gain is zero. Thus, any dc component in the input current would not show up in the induced current. The induced current between 0.1 to 100 Hz. can be regarded as a step signal, the response of which would be an exponential decay in time domain.

3. Contact resistance (ground mat resistance in case of ac and electrode resistance in dc transmission with ground return) can affect the magnitude of the induced currents as well as its decay time. An increase in contact resistance value would tend to reduce the magnitude of induced current slightly and also its decay time.
4. The presence of ground wires in a multiconductor system with ground return does not have any appreciable effect on the induced currents in the lines at low frequencies.
5. For simplicity and better understanding, the analysis was being carried out on a simple two conductor system with ground return. Various parametric studies are possible with the program developed in this thesis. Some of them have been explained in detail in Chapter 4.
6. A similar induced current as to that observed can be explained with the help of assuming a mutual contact resistance between the lines. This, however, leads to a finite induced current even at exactly zero frequency (dc) which is against the observed facts. This explanation must thus be discarded.

5.2 Recommendations for further work

1. Though in this thesis a simple multiconductor system is analyzed but a more complex system can be handled on similar lines. The model and the simulation program developed here could be extended for this purpose. The program has been developed to handle any number of conductors, and this exercise is thus quite straight forward.

2. Series capacitors in an ac transmission line could help in blocking direct currents from dc ground return transmission. Though there is no record to date of installing these series capacitors for such a purpose, a study can be carried out in this regard.
3. The direct induced current flowing through the neutral of the transformer could also be reduced by grounding neutrals of the transformer through a resistance of a few ohms. An exact analysis can be done in this respect.

REFERENCES

- (1) Carson, J. R., 'Wave Propagation in Overhead Wires, with Ground Return', Bell System. Tech. J., 192 , Vol. 5, pp 539-554
- (2) Shelkunoff, S. A., 'The electromagnetic theory of Co-axial transmission lines and cylindrical shields', Bell System. Tech. J., 1934, Vol. 13, pp 532-579
- (3) Sunde, E. D., 'Earth Conduction Effects in Transmission System', Princeton, N. J.: Van Nostrand, 1948.
- (4) Wedepohl, L. M. and Wilcox, D. J., 'Transient Analysis of Underground Power Transmission Systems', Proc. IEE, 1973, Vol. 120, No. 2, pp 253-260
- (5) Galloway, R. H., Shorrocks, W. B. and Wedepohl, L. M., 'transmission lines', Proc. IEE, 1964, Vol. 111, No. 12, pp 2051-2059
- (6) Deri, A., Tevan, G., Semlyen, A., and Castanheira, A., 'Homogeneous and Multi-Layer Earth Return', Trans. IEEE, Power System Apparatus; 1981, pp 3686-3693
- (7) Hedman, D. E., 'Propagation on Overhead Transmission lines I - Theory of Modal Analysis', Trans. IEEE (PAS), 1965, pp 200-205
- (8) Wedepohl, L. M., 'Electrical Characteristics of polyphase transmission system with special reference to boundary-value calculations at power line carrier frequencies', Proc. IEE, 1965, Vol. 112, No. 11, pp 2103-2112
- (9) Hedman, D. E., 'Propagation on Overhead Transmission Lines II - Earth Conduction Effects and Practical Results', Trans. IEEE, PAS, 1965, pp 205-211

- (10) Wedepohl, L. M., 'Application of matrix methods to the solution of travelling wave phenomenon in polyphase systems', Proc. IEE, 1963, Vol. 110, No. 12, pp 2200-2212
- (11) Kimbark, E. W., 'Direct Current Transmission', Vol. 1, John Wiley, 1971, pp 391-482
- (12) Gonzalez, R. C. and Wintz, P., 'Digital Image Processing', Addison-Wesley, 1977, pp 78-88
- (13) Wedepohl, L. M., 'Class notes on Transmission Lines course offered at the University of Manitoba', Winnipeg, 1986

APPENDIX-I

**(Excerpts from Minutes of Meeting held at System Performance Section
of Manitoba Hydro)**

The disturbance of September 18, 1985 @ 1:20

During paralleling tests of bipoles 1 and 2 lines at Grand Rapids tripped on two occasions on August 14, 1985 and September 18, 1985. On each occasion, lines tripped at Grand Rapids end only by the line high set instantaneous neutral overcurrent relays.

Due to the similarity of these disturbances and the unavailability of transient recorder charts from Grand Rapids for August 14, 1985, the disturbance of September 14, 1985 @ 1:20 is only analyzed here.

- (a) System Initial Conditions for the disturbance on September 18, 1985 @ 1:20 were:
- (i) Pole 1 and pole 2 had 3 valve groups each in service.
 - (ii) Pole 3 and pole 4 had 1 and 2 valve groups respectively.
 - (iii) D.C. powers on bipoles 1 and 2 were 6800 MW and 360 MW respectively at Dorsey.
 - (iv) Current orders on bipoles 1 and 2 were close to 800 and 500 Amps respectively.

(v) Poles 2 and 4 were in parallel mode on line DC2.

(b) Sequence of Events

$t = 0^-$ - a.c. undervoltage protection was operated manually on pole 4 at Dorsey.

$t = 0^+$ - Bypass pair (like a d.c. short) was formed on pole 4.

- $I_{dref} = 0$ and force retard signals were sent to Henday and Radisson from Dorsey for the paralleled poles 4 and 2.

$t = 20-30 \text{ msec}$ - $I_{dref} = 0$ and force retard commands received at Henday and Radisson. (Telecom delay)

$t = 90 \text{ msec}$ - parallel poles 4 and 2 blocked.

$t = 125 \text{ msec}$ - lines G1A and G2A tripped.

2. Discussion:

On September 2, 1985 @ 1:20, pole 2 of bipole 1 and pole 4 of bipole 2 were operating in parallel. To check the deparalleling sequence and the d.c. link response during deparalleling, an a.c. undervoltage protection on pole 4 was operated manually.

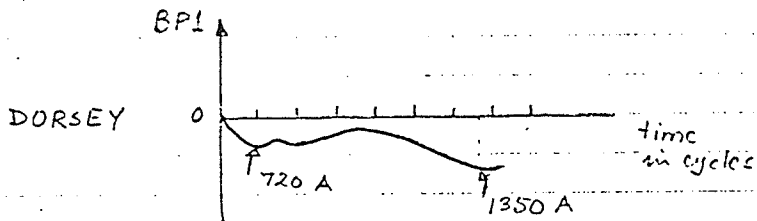
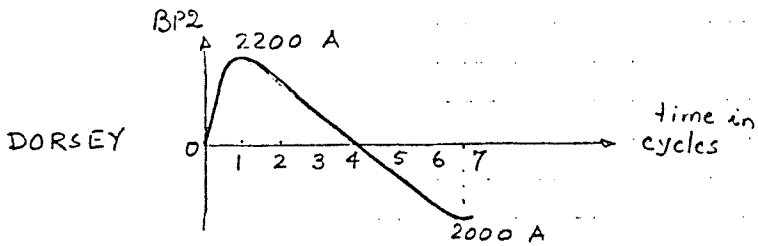
Operation of the undervoltage protection caused the formation of bypass pair on pole 4 valve groups at Dorsey. This in turn initiated $I_{dref} = 0$ signal for pole 4 and force retard signal for pole 2 which were then sent to pole 4 and pole 2 controls at Henday and Radisson respectively. Before these signals were received (telecom delay of 20-30 msec) by the respective stations, the

rectifiers of paralleled poles 4 and 2 fed large currents into the bypass pair on pole 4 at Dorsey. The initial current rise was largely limited by the impedances of the d.c. line D2, the line reactors of poles 2 and 4 at Radisson and Henday and the line reactor of pole 4 at Dorsey. Later but before $I_{dref} = 0$ and force retard signals were received, the poles 4 and 2 controls at Henday and Radisson raised their firing angles in an attempt to bring their pole currents to the predisturbance levels. Increased currents and firing angles on paralleled poles caused a substantial reactive power demand on the collector system. The a.c. voltage in the collector system depressed momentarily. This was reflected in reduced currents on poles 3 and 1. After receipt of the $I_{dref} = 0$ and the force retard commands on poles 4 and 2 at Henday and Radisson, currents on poles 4 and 2 started to reduce, a.c. voltage started to recover and the currents on poles 3 and 1 started to increase. In about 5-6 cycles after the bypass pair formation, currents on poles 4 and 2 became zero. The currents however continued to increase on poles 3 and 1 to satisfy power orders of their bipoles. In so doing the current on poles 3 and 1 experienced a large overshoot (60% of the final value) in about 2-3 cycles after current zero on poles 4 and 2. It appears that the large overshoot in the non paralleled pole currents were influenced by the following factors:

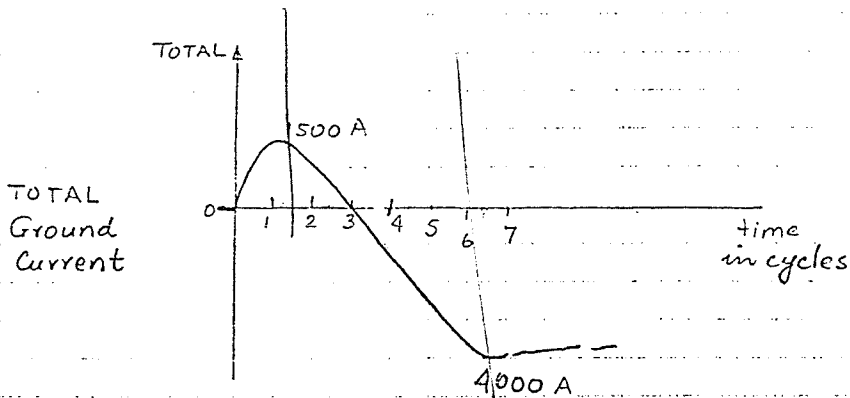
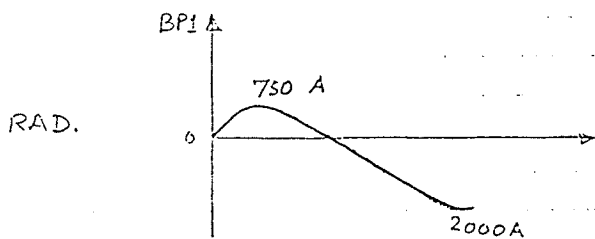
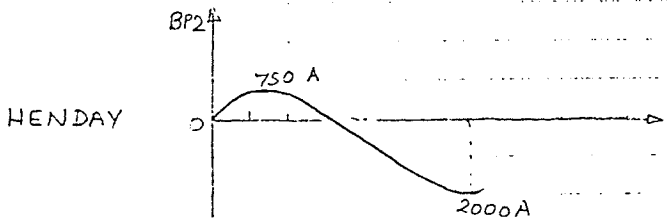
- (i) Bipoles 1 and 2 power orders
- (ii) No. of valve groups in operation on unparallelled poles
- (iii) dynamic response of poles 1 and 2

FIGURE 2

GROUND CURRENTS OF BIPOLES 1 & 2
AND THEIR TOTAL



Note: Current values are derived from the Hathaways of BP1 & BP2



(iv) a.c. voltage transients in the collector system

Following the formation of bypass pair on pole 4, the collector system voltage depressed as discussed earlier and therefore the firing angles on the nonparalleled poles moved close to 5° . When the currents on the parallel poles 4 and 2 came down to zero, the a.c. voltage in the collector system rose with an overshoot. With rectifiers at 5° , nonparalleled poles experienced an overshoot larger than the normal.

Figure 2 shows the waveshape of the d.c. ground electrode current (difference in the pole currents) for each dipole during the disturbance. It shows that the ground current was zero before the bypass pair was formed on pole 4 at Dorsey. The total ground current of the two bipoles increased to a maximum of 1500 Amp in about 1 cycle, came down to zero in another 3-4 cycles and reached a maximum of 4000 Amp in the direction opposite to the first maximum.

Figure 3 shows the 230 kV bus voltage and the transient current changes on the transformer neutral and lines at Grand Rapids ends. The transient current waveshapes look identical to the total ground current waveshape produced by the d.c. A comparison of figures 2 and 3 indicates that each of the G1A, G2A and G9P lines had approximately one-fifth of the d.c. ground current.

Conclusions:

Whatever may be the cause, the test and the disturbance present the following facts:

- (i) Large neutral currents (which tripped lines at Grand Rapids on August 14, 1985 @ 03:00 and September 18, 1985 @ 01:20) can occur on all the lines parallel to the HVDC line only when two poles are in the parallel mode of operation.
- (ii) Fault at Dorsey on the d.c. line associated with the paralleled poles cause a maximum ground current of 2 000 Amps on the d.c. and following the block of the paralleled poles, the ground current goes to another maximum with reverse polarity. The second maximum depends on the power orders of each bipole and the number of valve groups on the nonparalleled poles. This maximum can be close to 6 500 Amp (with current orders of 2 000 Amps on each bipole and an overshoot of 60%).
- (iii) The neutral current on the lines A3R, A4D, G1A, G2A and G8P seem to follow the shape of the d.c. ground current. The maximum neutral current on each of G1A, G2A and G8P lines which have caused lines at Grand Rapid to trip is close to one-fifth and on each of A3R and A4D is close to one-sixth of the d.c. ground current. For an estimated 6 500 Amp maximum d.c. ground current, the neutral current on each of the lines G1A, G2A and G8P can be expected to be 1 300 Amps and 1100 A on each of A3R and A4D.
- (iv) When one of the lines G1A and G2A is out of service the line in service experiences nearly 1.75 times the neutral current than if both lines were in service. G8P neutral current is not affected by the outage of either G1A or G2A line. The maximum current when one of the lines G1A or G2A is out of service can therefore reach 2 300 Amps. It is also expected that when A3R or A4D is out of service the line in service could experience a neutral current of about 1 900 A.

(v) All these observations do not lead to prove the cause as either the ground current or the induction theory can explain the observed phenomena.

(vi) Monitoring of the open line voltage at Ashern in Test #2 is therefore essential to establish the cause.